Focused Workshop on Rare Isotope Physics,
Yeosu Expo Convention Center, Korea, 24-26 November 2022

Plan to study the nuclear equation of state and symmetry energy at RAON

Byungsik Hong

Center for Extreme Nuclear Matters (CENuM), Korea University

for the LAMPS Collaboration

Outline

1. Introduction to EoS & symmetry energy
2. Observables
3. LAMPS
4. Low-energy detectors
5. Summary

Part 1.

Introduction to EoS & symmetry energy

Phase diagram of ordinary matter

- **States or Phases:** Solid (ice), Liquid (water), Gas (vapor)

Phase diagram of H_2O

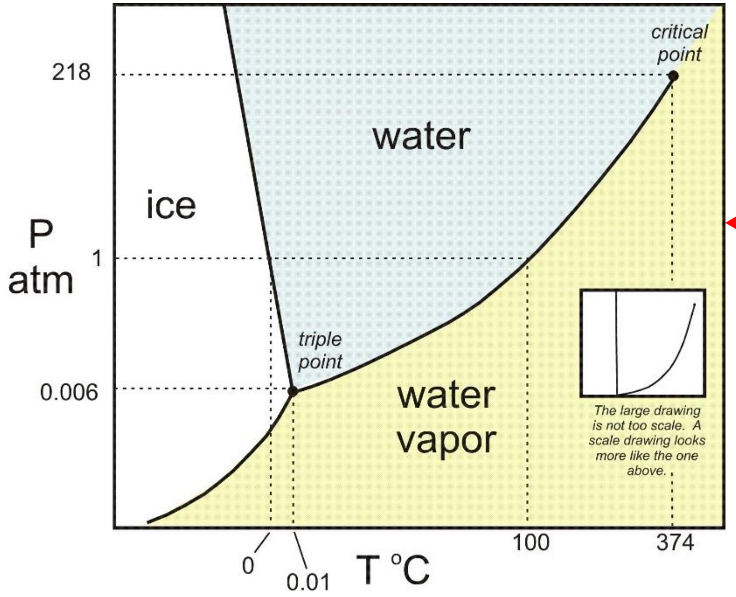

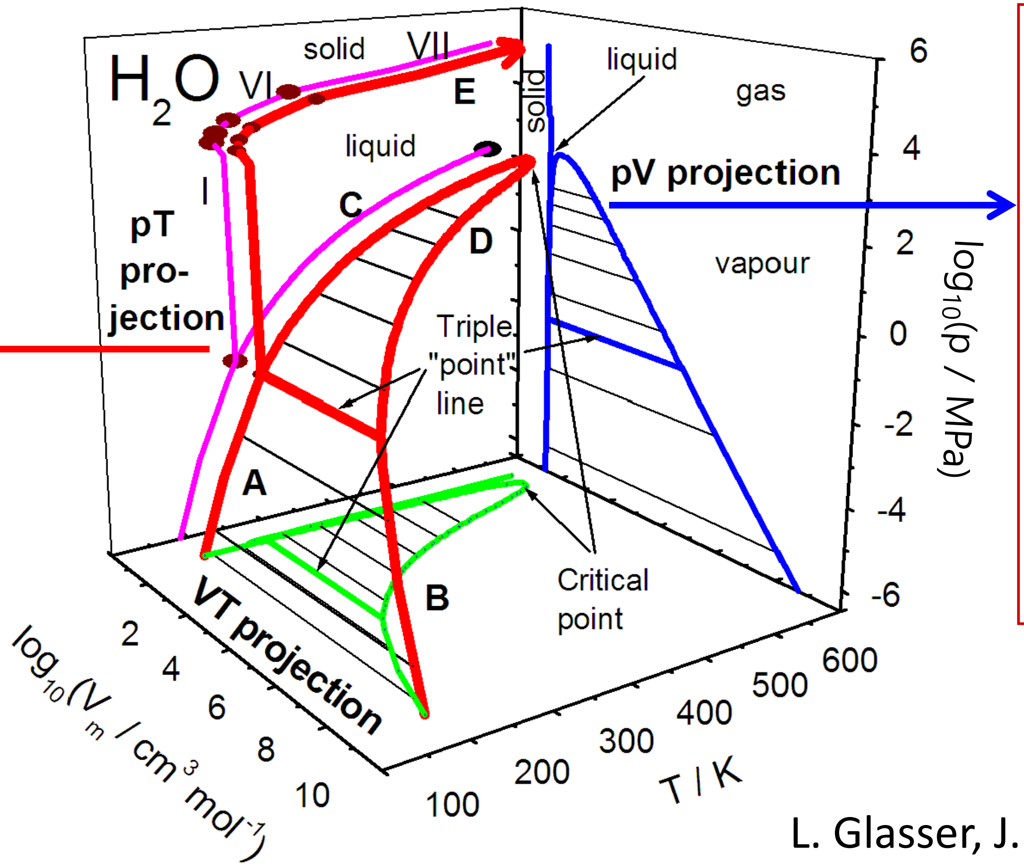

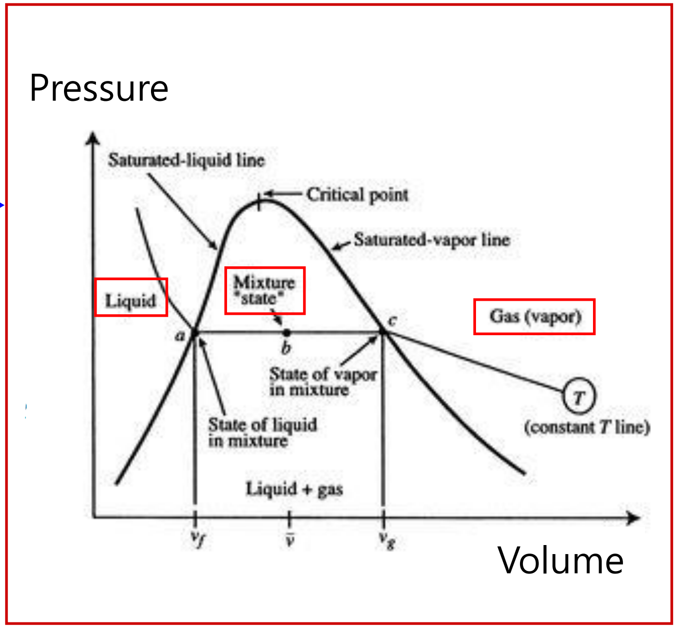

L. Glasser, J. Chem. Educ. 81, 414 (2004)

Equation of state of ordinary matter

- Definition of the equation of state (EoS)
  - The relation among the thermodynamical variables such as pressure (p), temperature ($\tau = k_B T$), and volume (V) to describe the state of matter
- Basic examples
  - Vapor pressure equation (or Clausius-Clapeyron equation)

    $dp/d\tau = L/\tau\Delta v$ (L: latent heat, Δv: the volume change when one molecule is transferred from liquid to gas)

    $\longrightarrow p(T) = p_0 \exp(-L/N_0\tau)$ for $v_g \gg v_l$ and $pV_g = N_g\tau$
  - Van der Waals equation of state: The simplest model of a liquid-gas phase transition

    $(p + N^2 a/V^2)(V - Nb) = N\tau$

    where

    a: long-range attraction between two molecules

    b: short-range repulsion between two molecules

    [Ref.] Undergraduate textbook, e.g., “Thermal Physics” by C. Kittel & H. Kroemer

Phase diagram of nuclear matter

Variables: $(p, V, \tau) \;\rightarrow\; (\rho, \tau)$ with the net baryon density ρ

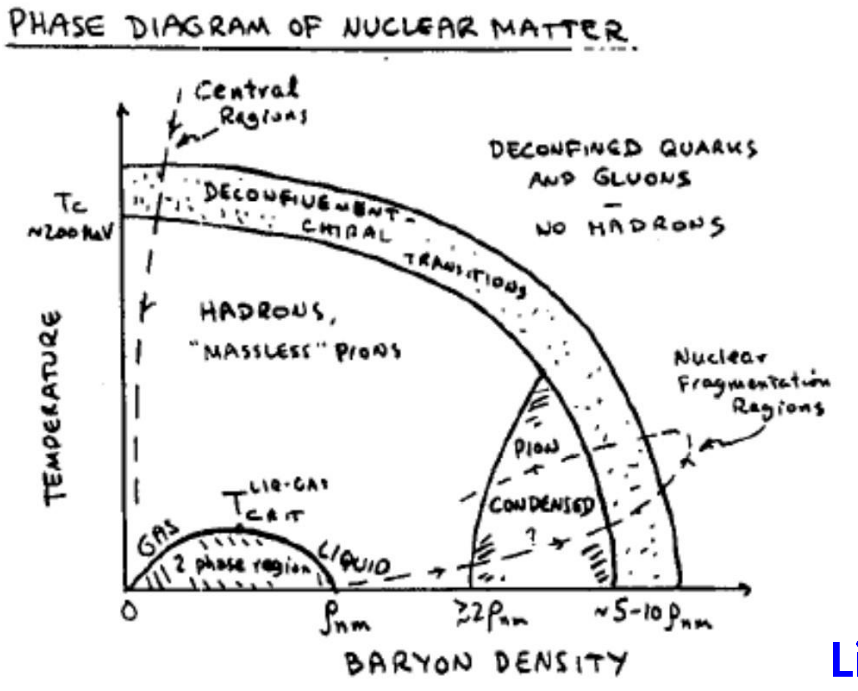

NSAC Long Range Plan Report (1983)

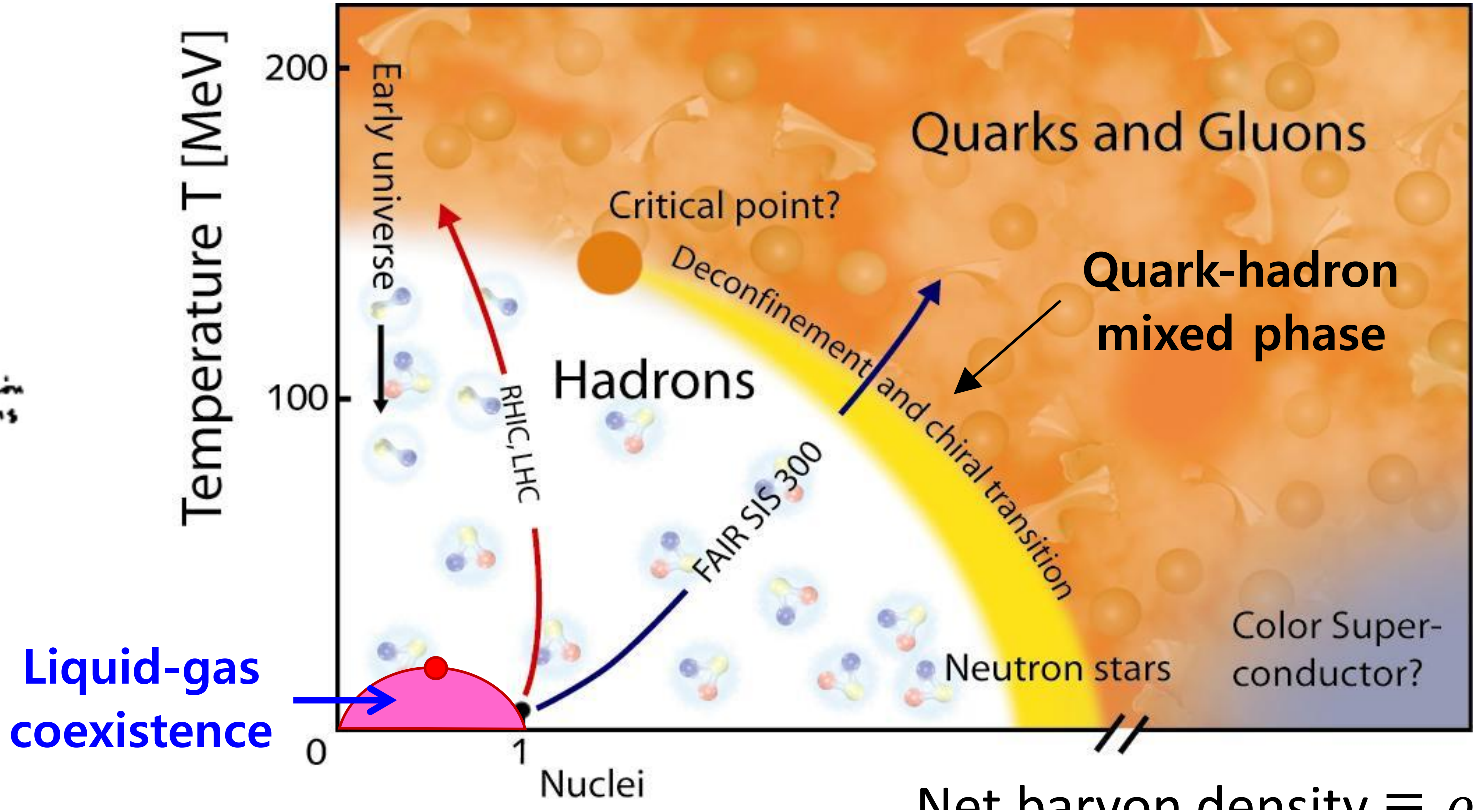

Net baryon density $\equiv \rho/\rho_0$
(Sometimes people use μ_B)

Equation of state of nuclear matter

- One of the possible EoS's, using the differential thermodynamic identity, can be

$$p(\rho,\tau,\delta) = -\left[\frac{\partial F}{\partial V}\right]_{\tau,\delta} ; F(\rho,T,\delta) = U(\rho,T,\delta) - \tau\cdot\sigma(\rho,T,\delta)$$

F = Helmholtz free energy, U = Average energy of the state, σ = Entropy

$\rho = \rho_n + \rho_p$: Total baryon density, $\delta = (\rho_n - \rho_p)/(\rho_n + \rho_p)$: Isospin asymmetry

- Using the baryon density $\rho = A/V$ and $\partial V = -A\cdot\partial\rho/\rho^2$,

$$p(\rho,\tau,\delta) = -\left[\frac{\partial F}{\partial V}\right]_{\tau,\delta} = \left[\rho^2\frac{\partial(U(\rho,\tau,\delta)/A)}{\partial\rho}\right]_{\tau,\delta} - \left[\tau\rho^2\frac{\partial(\sigma/A)}{\partial\rho}\right]_{\tau,\delta}$$

  - At low temperatures, the second term becomes negligible.

- Practical approach is to calculate the average energy per nucleon for EoS

$$\varepsilon(\rho,\tau,\delta) \equiv U(\rho,\tau,\delta)/A$$

  - Theoretical approach: Estimate $\varepsilon(\rho,\tau,\delta)$ by some density functional forms (e.g., Hartree-Fock) and variational calculations.
  - Experimental approach: Constrain EoS by using the controlled Lab. Expts. at specific densities.

Equation of state and symmetry energy

- Total energy of nuclei or nuclear matter

$$\varepsilon(\rho,\delta)A = Zm_p + Nm_n - B(A,Z)$$

with

$$B(A,Z) = a_{vol}A - a_{sur}A^{2/3} - a_{Coul}\ Z(Z-1)/A^{1/3} - a_{sym}\,(N-Z)^2/A \pm \delta_{pair}$$

$$\therefore\ \varepsilon(\rho,\delta) = \varepsilon(\rho,\delta=0) + E_{sym}(\rho)\delta^2 + \mathcal{O}(\delta^4) + \cdots$$

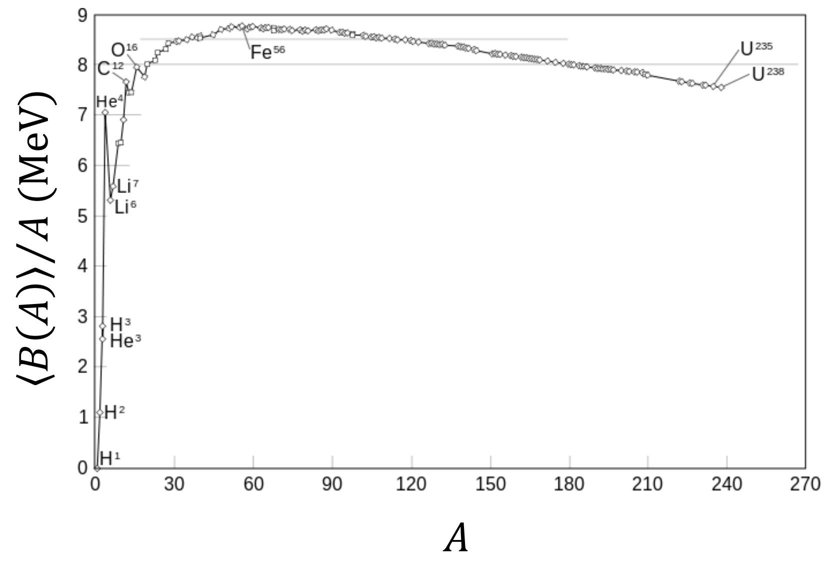

- Symmetry energy E_{sym}
  - The energy difference between the neutron matter and the isospin symmetric matter
  - $a_{sym} \approx E_{sym}(0.6\rho_0)$
  - Primary concern is the density dependence of E_{sym}.

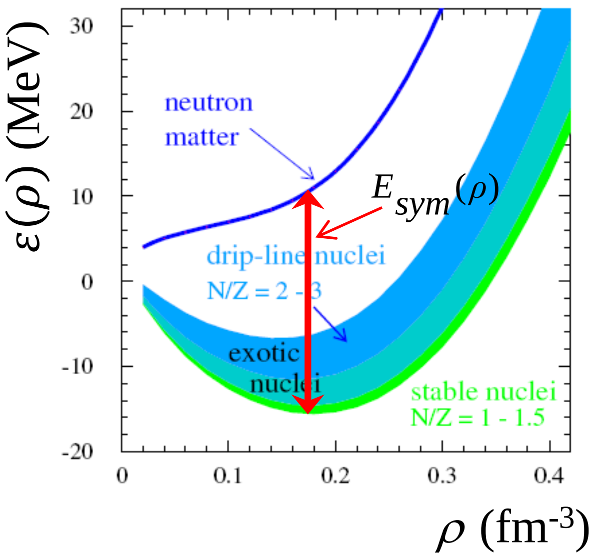

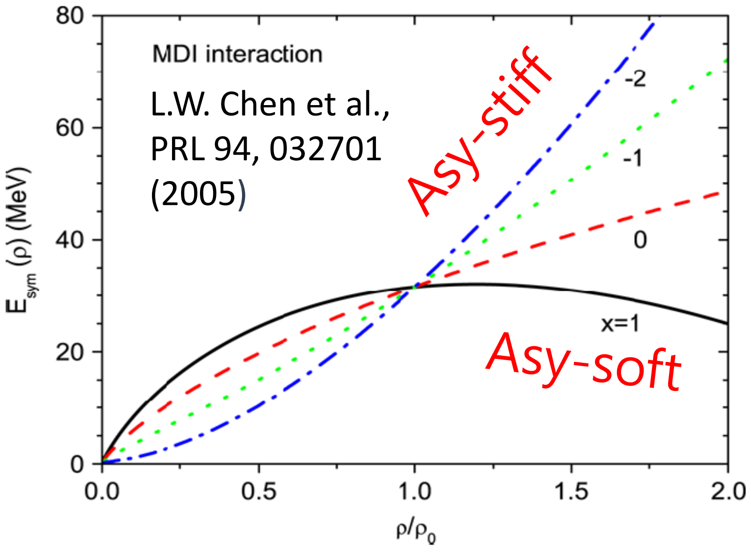

Symmetry energy

- Two components of the symmetry energy

$$E_{sym}(\rho) = S(\rho) = \frac{1}{3} E_F \, (\rho\, /\rho_0)^{2/3} + E_{sym}^{pot}(\rho)$$

where $E_{sym}^{pot}(\rho)$ is often parameterized as $C(\rho\, /\rho_0)^{\gamma}$

- A useful empirical expansion around ρ_0:

$$E_{sym}(\rho) = S_0 + \frac{L}{3}\left(\frac{\rho-\rho_0}{\rho_0}\right) + \frac{K_{sym}}{18}\left(\frac{\rho-\rho_0}{\rho_0}\right)^2$$

$$L = \frac{3}{\rho_0} P_{sym} = 3\rho_0 \frac{\partial E_{sym}(\rho)}{\partial \rho}\bigg|_{\rho=\rho_0} \quad \left(\text{slope} \leftrightarrow \text{pressure}\right)$$

$$K_{sym} = 9{\rho_0}^2 \frac{\partial^2 E_{sym}(\rho)}{\partial \rho^2}\bigg|_{\rho=\rho_0} \quad \left(\text{curvature} \leftrightarrow \text{compressibility}\right)$$

  - Important constraints on the nuclear effective interactions

- Present constraints on symmetry energy compiled by *H. Wolter*

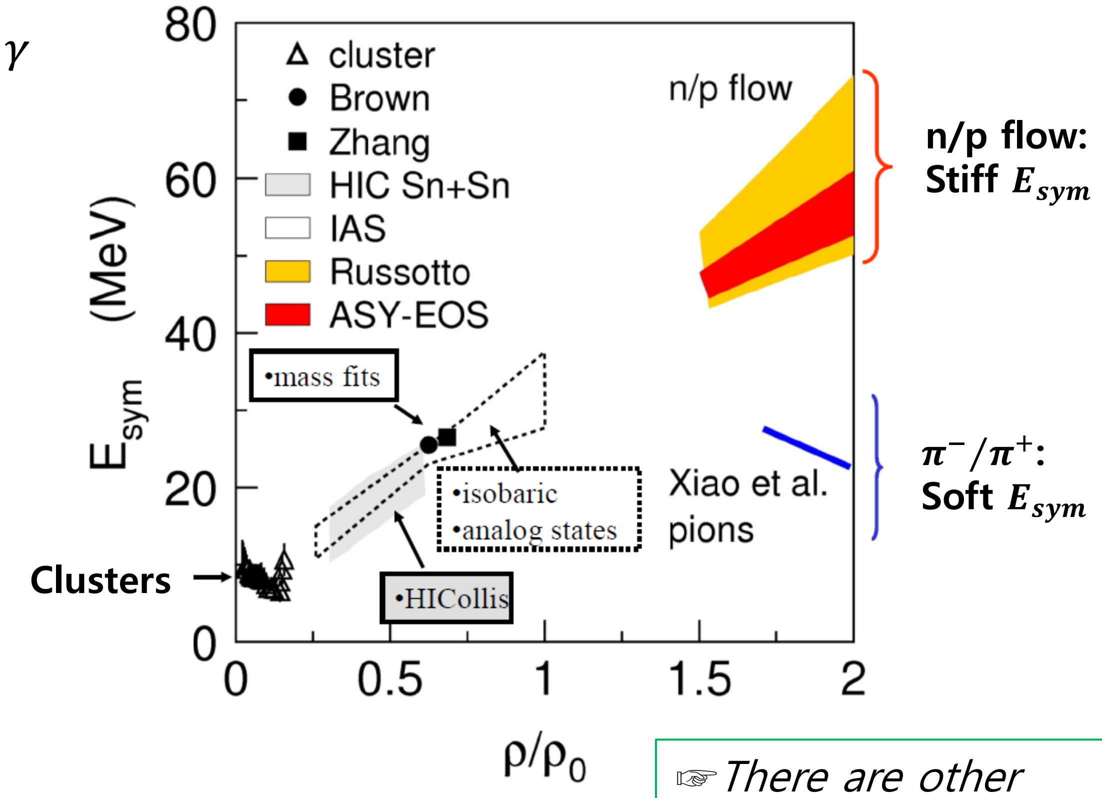

☞ *There are other predictions showing different trends.*

Symmetry energy and neutron stars

- Symmetry energy helps to understand
  - Stability of neutron stars against gravitational collapse
  - Stellar density profile and internal structure of neutron stars
  - M vs. R relationship of neutron stars
    - Sensitive to EoS and E_{sym}
  - Various observational consequences such as
    - Cooling rates of proto-neutron stars
    - Stellar masses, radii & moment of inertia from temperatures & luminosities of X-ray bursters
- We need to provide ***systematic constraints from the controlled laboratory experiments*** at specific ρ's.

J.M. Lattimer,
Ann. Rev. Nucl. Part. Sci. 62, 485 (2012)

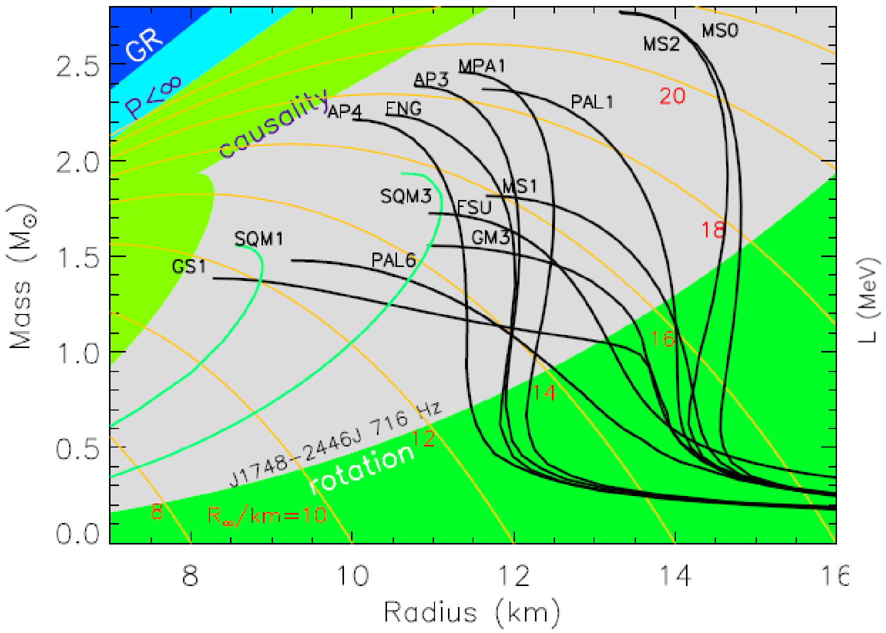

J.M. Lattimer & Y. Lim,
ApJ 771, 51 (2013)

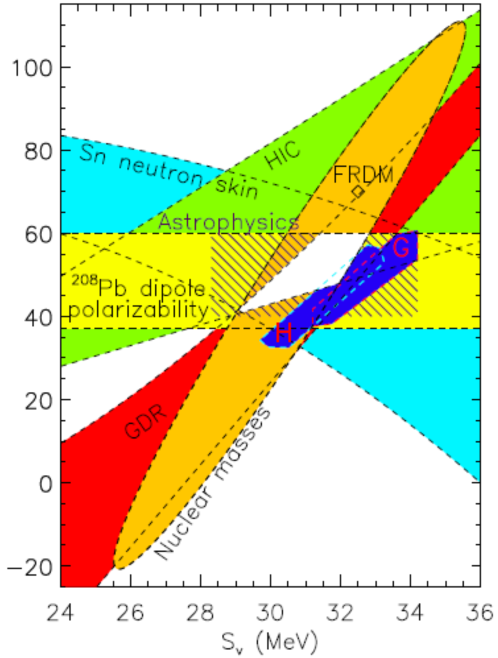

- Black line: Hadronic EOS
- Green line: SQM EOS
- GR: Excluded by general relativity
- $\mathrm{P} < \infty$: Excluded by requiring finite pressure
- Causality: Excluded by causality
- Rotation: Bounded by realistic mass-shedding limit for the highest known pulsar frequency

Phase diagram of nuclear matter with RIB

Variables: $(p, \tau, V) \rightarrow (\rho, \tau, \delta)$

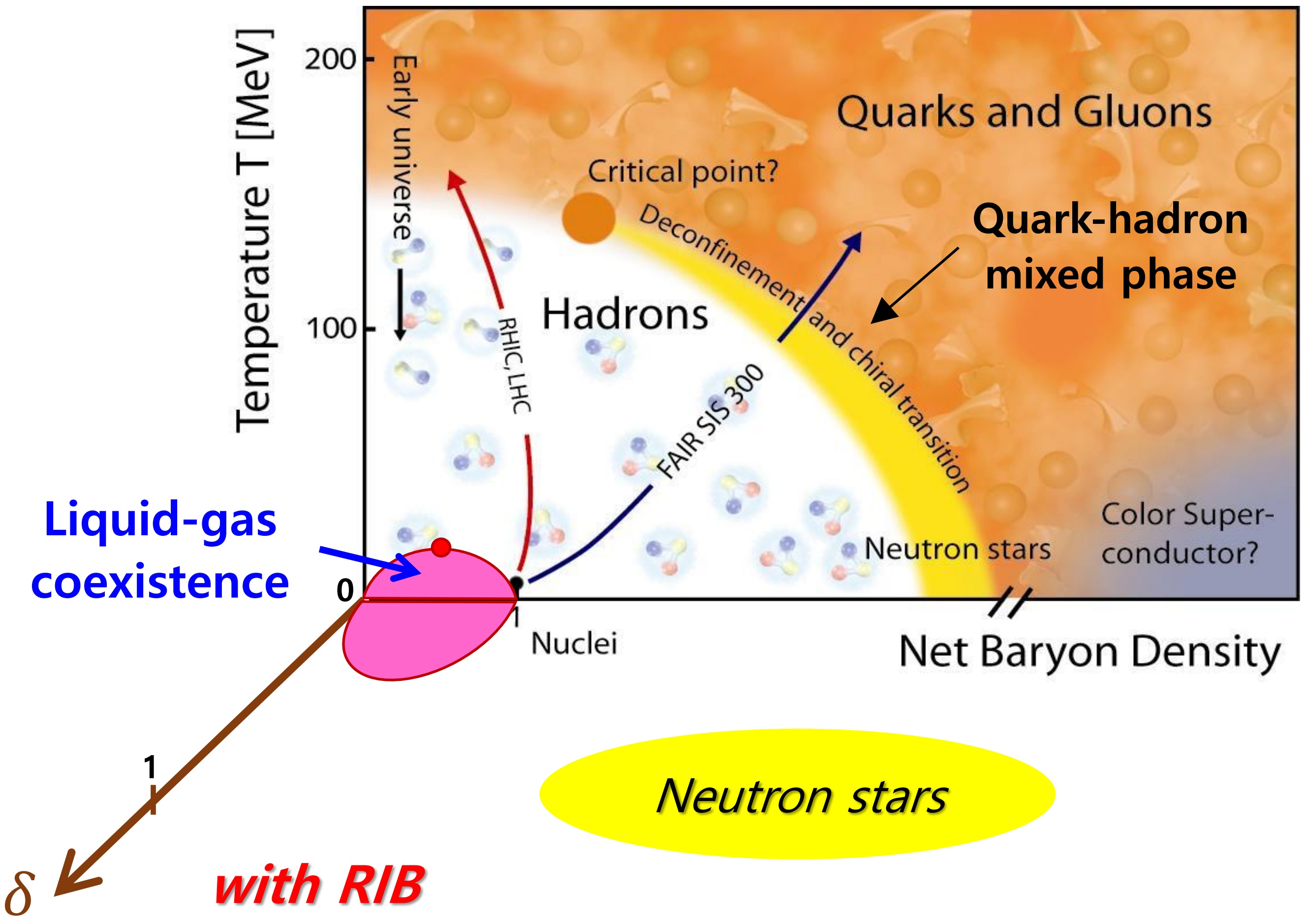

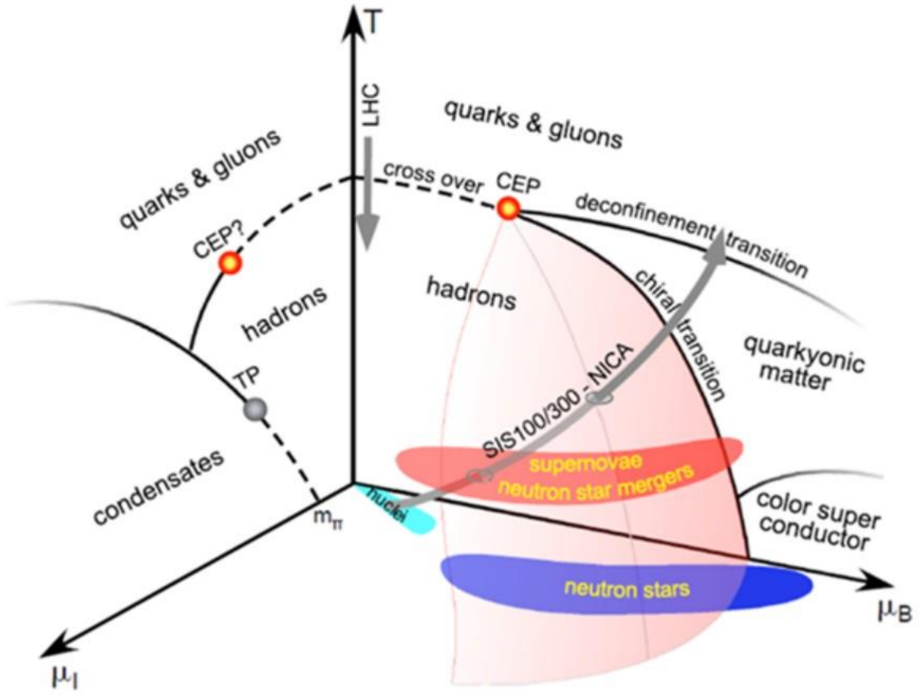

http://cbm.gsi.de

Part 2.

Observables

Observables sensitive to symmetry energy

- Hadronic observables
  - Particle spectra and yield ratios for n/p, $^{3}H/^{3}He$, $^{7}Li/^{7}Be$, π^{-}/π^{+}, etc.
  - Collective flow: v_1 & v_2 of n, p, and fragments
  - Azimuthal angle dependence of n/p ratio relative to the reaction plane
  - Isoscaling phenomenon in nuclear multi-fragmentation process
    (Jung Woo Lee in this Workshop)
  - Isospin transportation: isospin diffusion and migration (or drift)
- Electromagnetic observables
  - Dipole ($E1$) emissions (pygmy and giant dipole resonances): peak position and magnitude
    - Some theories suggest that PDR is sensitive to the neutron skin radius for unstable nuclei.
  - Angular dependence of the gamma emission
- Systematic investigation for the EoS and symmetry-energy experiments
  - Change of the system size and N/Z of the collision system
  - Change of the beam energy to cover a wide range of ρ/ρ_0
  - Analyze any variable as functions of the collision centrality and kinetic energy

Isospin transportation

- Difference between neutron and proton currents

$$j_n - j_p \propto \delta \left(\frac{\partial E_{sym}}{\partial \rho} \right) \nabla \rho - \rho E_{sym} \nabla \delta$$

  - $\nabla\delta$ effect (isospin diffusion): Asymmetric flow from projectile and target for isospin equilibration
  - $\nabla\rho$ effect (isospin migration or drift): Asymmetric flow from projectile and target towards low-density region (neck), which would be more important at Fermi energies and below

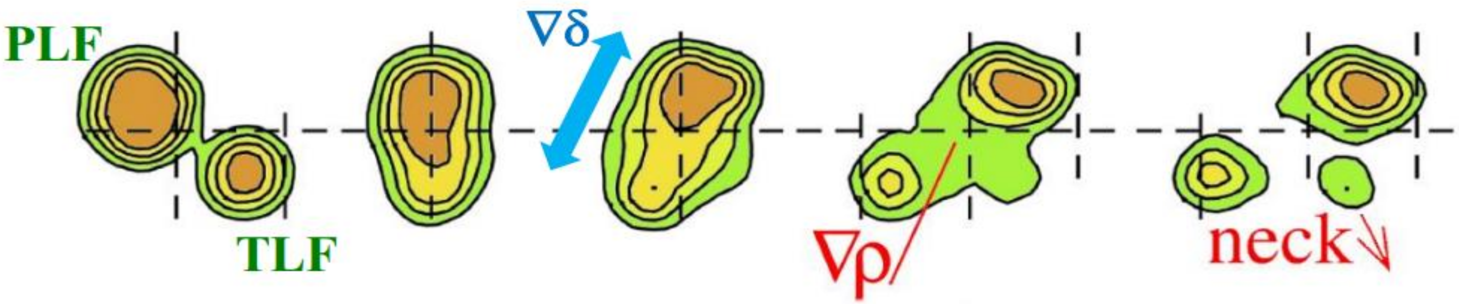

(from M. Colonna)

Isospin tracer parameter

FOPI Collaboration @ GSI
F. Rami et al., PRL 84, 1120 (2000)
B. Hong et al., PRC 66, 034901 (2002)

$$R_X = 2\frac{X^{AB} - (X^{AA} + X^{BB})/2}{X^{AA} - X^{BB}}$$

R_X = 0 for complete isospin mixing

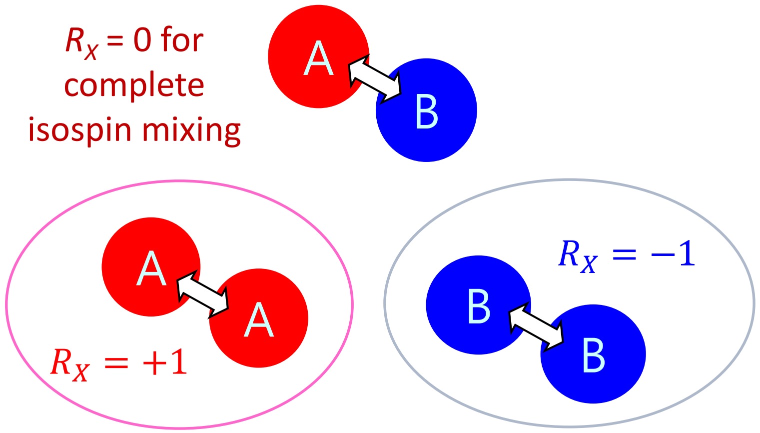

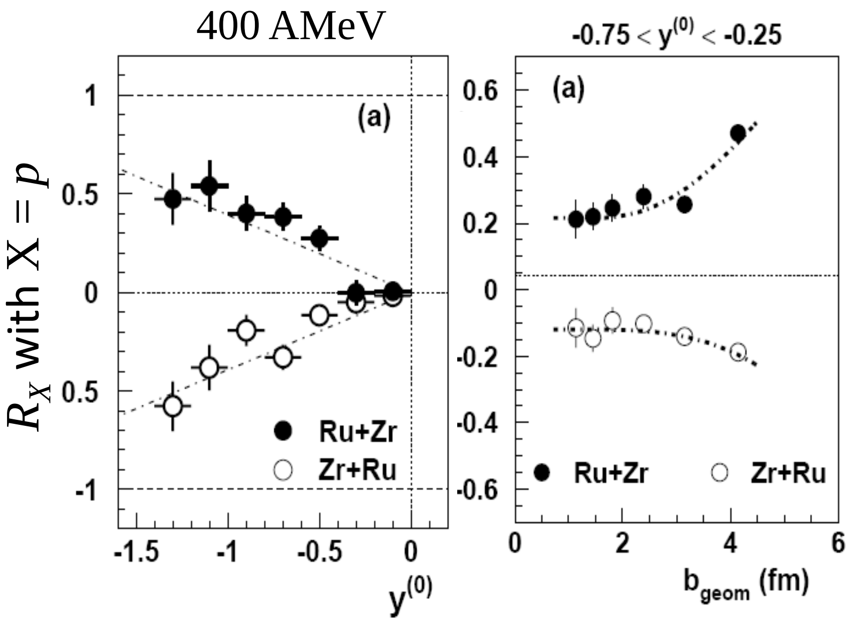

M.B. Tsang et al., PRL 92, 062701 (2004)

$$\frac{Y_{124+124}(Z=3\sim8)}{Y_{112+112}(Z=3\sim8)} \propto \exp(\alpha N)$$

α=Neutron-isoscaling parameter

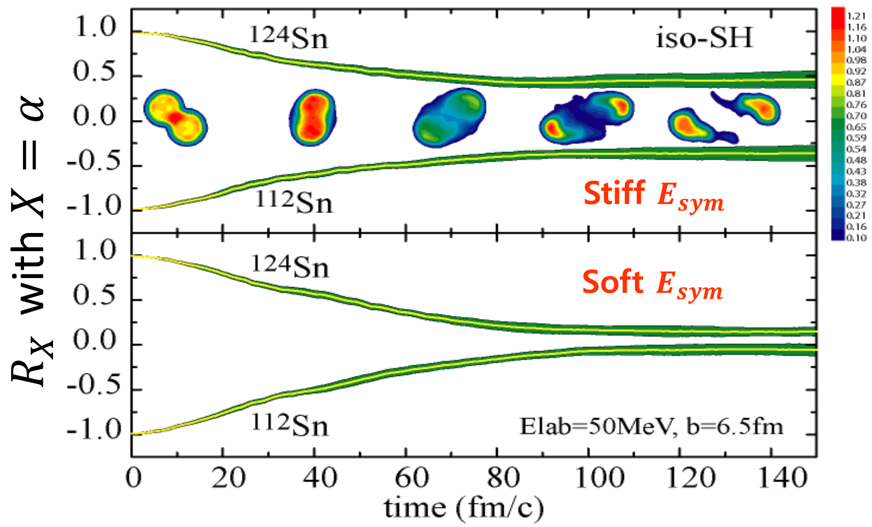

J. Rizzo et al., NPA 806, 79 (2008)
Stochastic Mean Field (SMF) Model

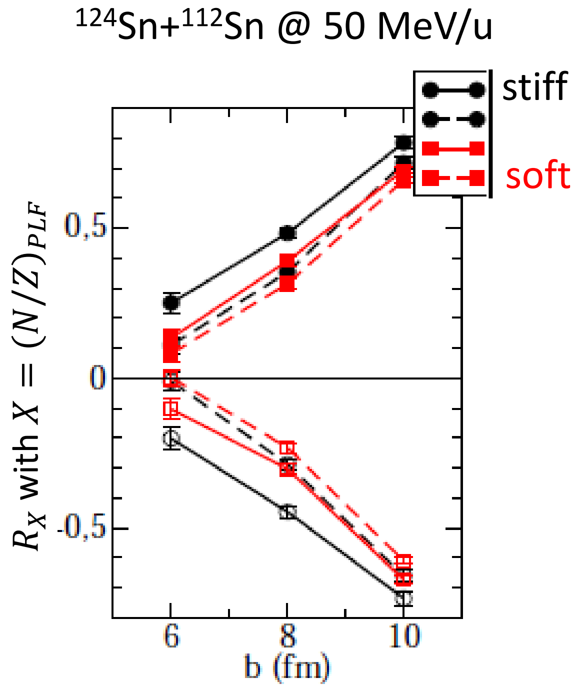

- Softer E_{sym} towards equilibrium ($R_X \to 0$)
- Models predict good sensitivity to E_{sym}

Recent hadron data from SπRIT

- SπRIT experiment @ RIKEN
  - SAMURAI + TPC for ^{108,112,124,132}Sn+ ^{112,124}Sn @ 270 AMeV
  - Results on $\pi^{\pm}$ yield ratio, production of Z=1 isotopes, and isoscaling phenomenon of light charged particles

PRL126, 162701 (2021)

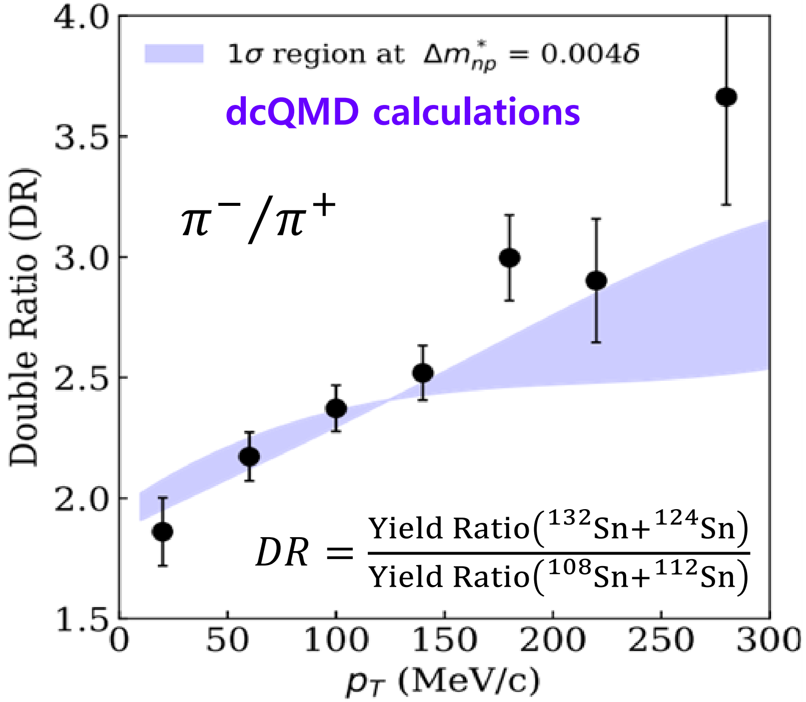

PLB822, 136681 (2021)

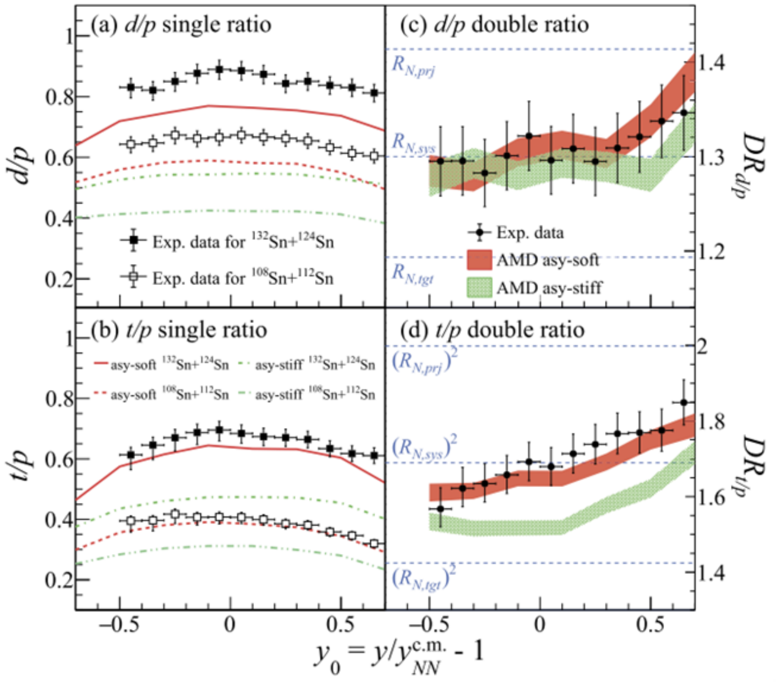

EPJA58, 201 (2022)

J. W. Lee in the next session

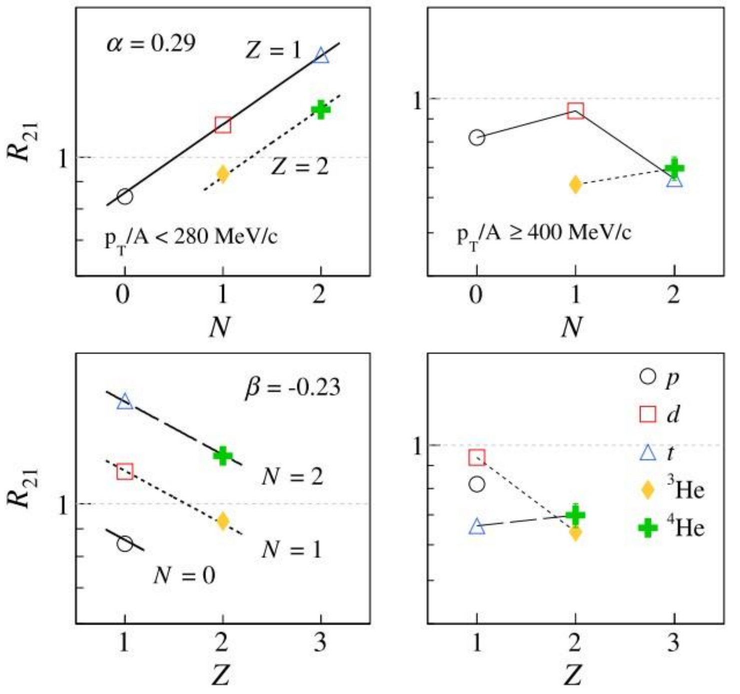

Dipole emission

- Origin of dipole ($E1$) emission depends on the beam-energy range
  - $\mathcal{O}(10\ \mathrm{MeV}/u)$: Oscillation in fusion
  - $\mathcal{O}(50\,\mathrm{MeV}/u)$: Diffusion
  - $\mathcal{O}(\sim 200\,\mathrm{MeV}/u)$: Nuclear structure (neutron skin, PDR, and GDR)
  - $\mathcal{O}(>200\,\mathrm{MeV}/u)$: Isospin equilibration in nuclear stopping
- PDR is sensitive to E_{sym}:

  → HF+RPA with various Skyrme potentials shows that a larger L gives a larger strength in the PDR region.
- It is necessary to study systematically using n-rich systems:
  - ^{X}Ca beams with X=50, 54, 60, …
  - ^{X}Ni beams with X=68, 70, 72, …
  - ^{X}Sn beams with X=112, 124, 130, 132, …

L = SGII (38 MeV) < SLy5 (48 MeV) < SkI3 (100 MeV)

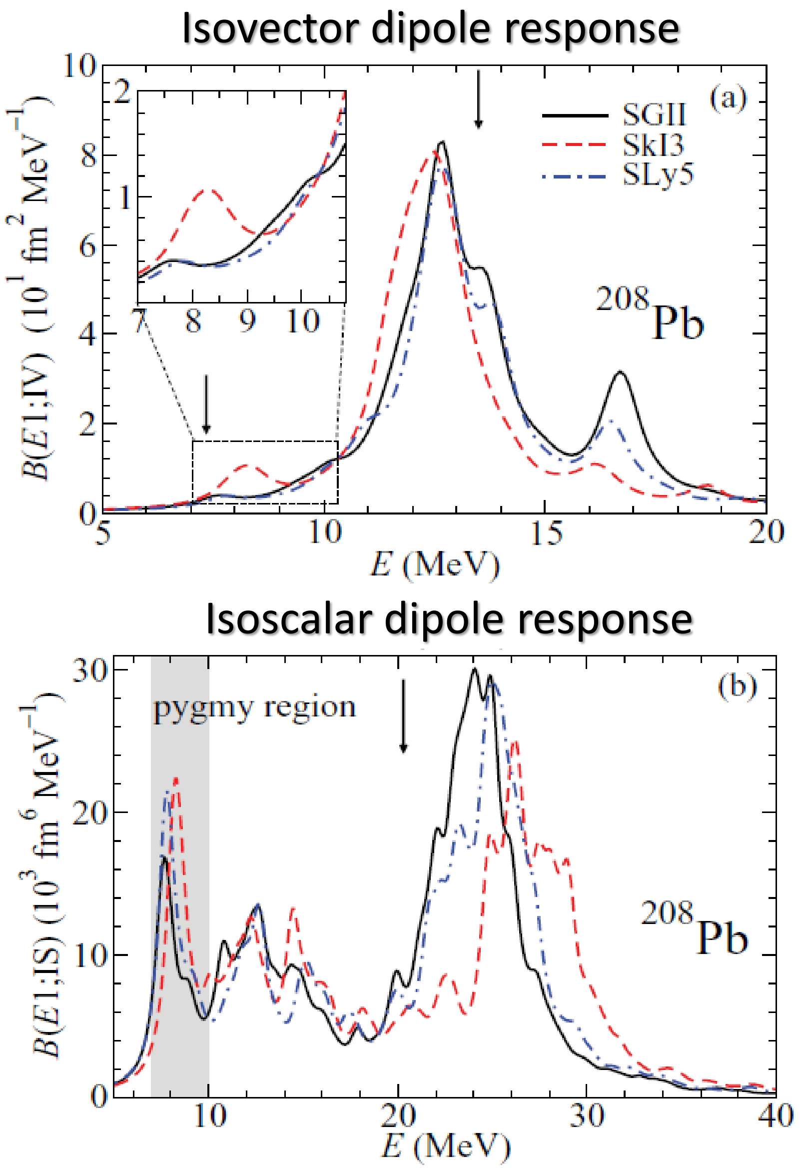

X. Roca-Maza et al., PRC85, 024601 (2012)

Dipole emission in fusion reactions

- Examples of the existing data
  - $^{X}Ar+^{96}Zr$ with X=36 (reference) and > 40
  - $^{X}S+^{100}Mo$ with X=32 (reference) and > 40
  - Model calculations assuming stiff and soft E_{sym} compared with the LNS data

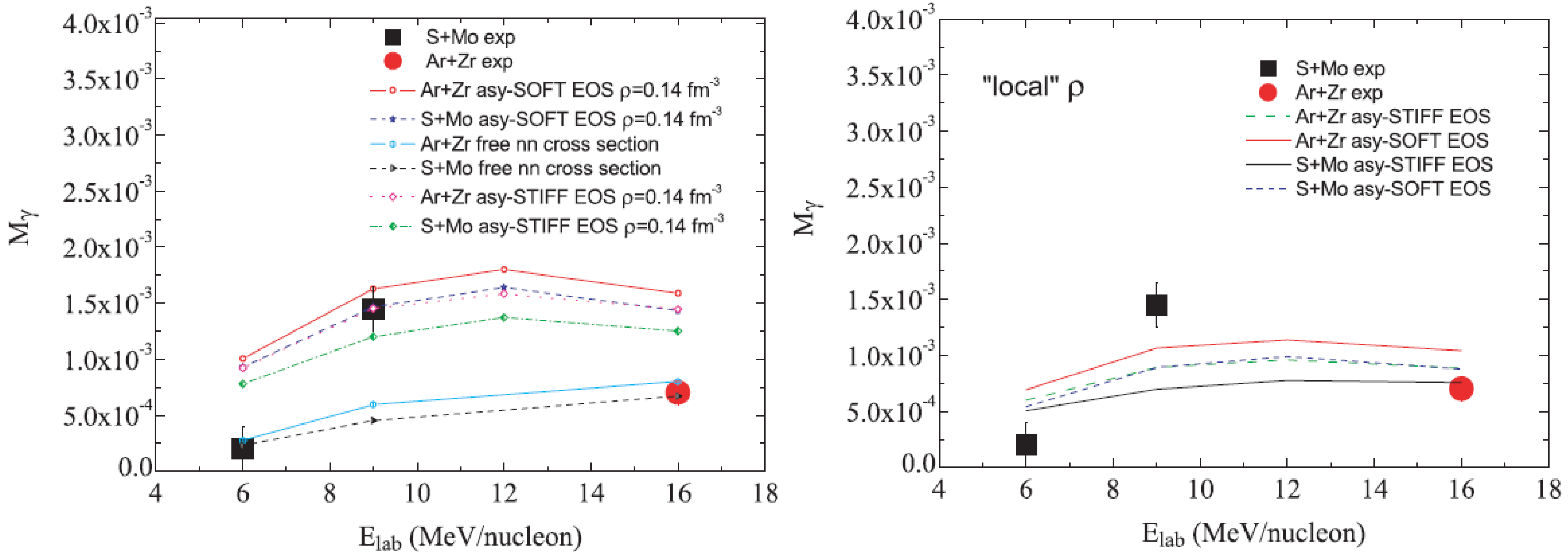

D. Pierroutsakou et al., PRC80, 024612 (2009)]

↙ Beam energy range of SCL3 at RAON

- We need the precise data, even for the light systems, on the dipole emission.

Symmetry pressure and radii

- Neutron skin (R_n) vs. E_{sym}
  - P_{sym} is larger if E_{sym} strongly varies with ρ:

$$P_{sym} = \rho_0^2 \frac{\partial E_{sym}(\rho)}{\partial \rho}\bigg|_{\rho=\rho_0}$$

$$P_{n-matter} = P_{symmetric-matter} + P_{sym}$$

  → Symmetry pressure repels neutrons and attracts protons: a stiff symmetry energy gives a larger radius for neutron skin.

  - Direct way to measure the neutron radius is using $A_{PV} = A_{LR} \sim A_{weak}/A_{\gamma}$ in $\vec{e} + \mathrm{A}$, for example, PREX/PREX-II/CREX experiments at Jefferson Lab. [PRL108, 112502 (2012)]
  - But there is no electron beam at RAON!

- Thus, we may take the indirect way:

  → Theoretical (e.g., RPA) prediction: A strong correlation between the difference between n & p radii and the fractional strength in PDR.

  - Measure the yield ratio s of PDR and GDR.

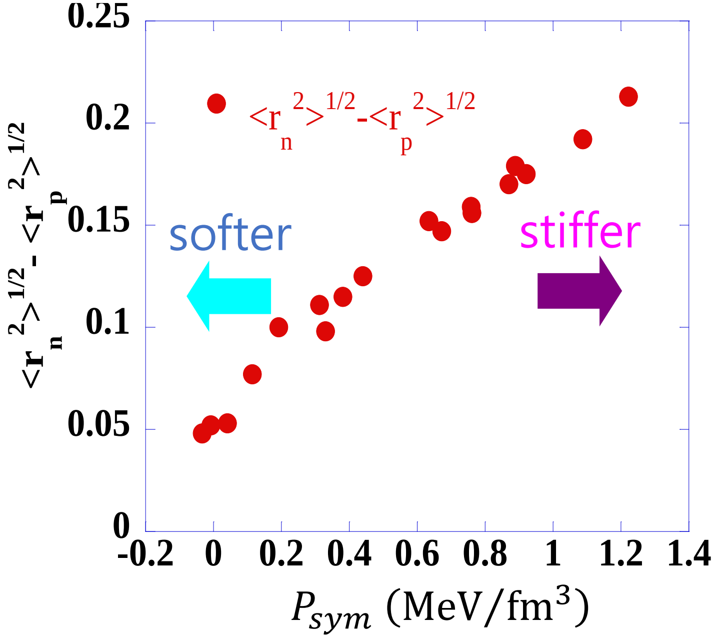

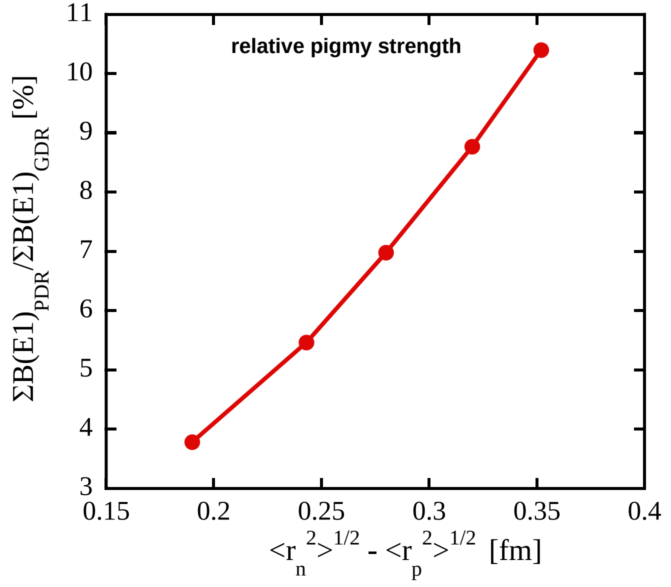

A. Klimkiewicz, et al., PRC76, 051603(R) (2007)

Dipole emission in n-rich nuclei

A. Carbone et al., PRC 81, 041313 (2010)

$L = 64.8 \pm 15.7$ MeV

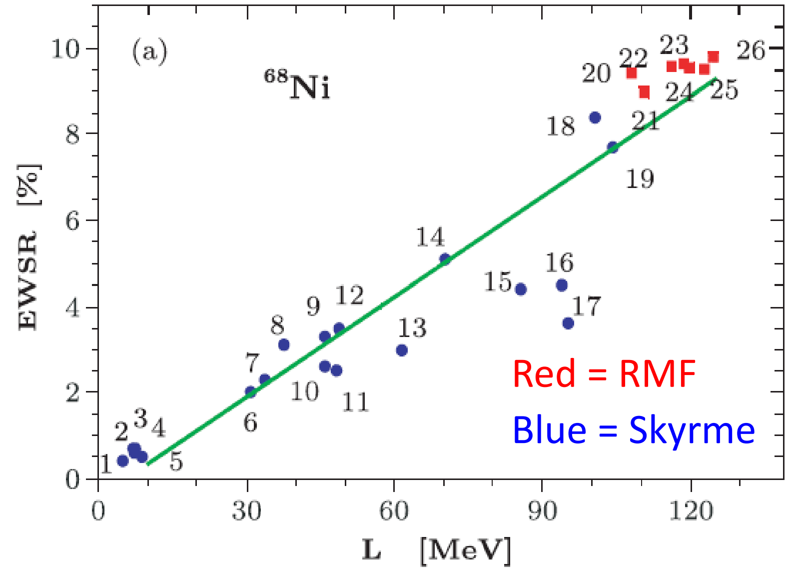

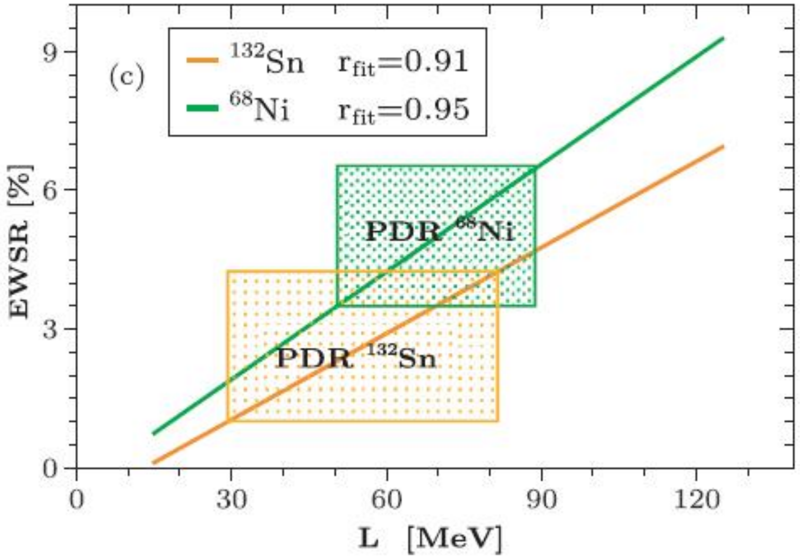

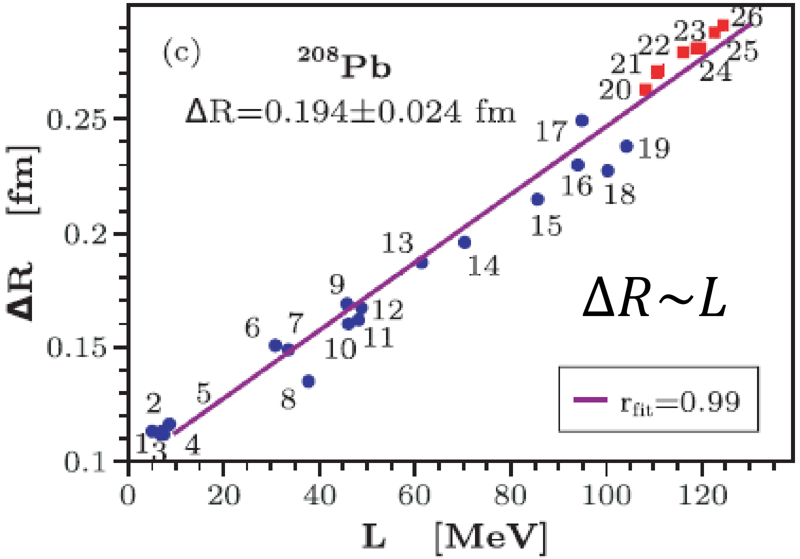

↑ Nuclear models show a strong correlation between the fractional dipole strength of PDR and symmetry pressure (or L).

- Required detectors for the EoS & symmetry-energy experiments
  - Beam diagnostic detectors for tracking and reference timing
  - Large acceptance tracking detector for the charged particles (from pions to fragments)
  - Neutron (and gamma) detectors
  - Event characterization detector for centrality & reaction plane

Part 3.

LAMPS:
Large Acceptance Multi-Purpose Spectrometer

Uniqueness of LAMPS

LAMPS can take all available beams at RAON!

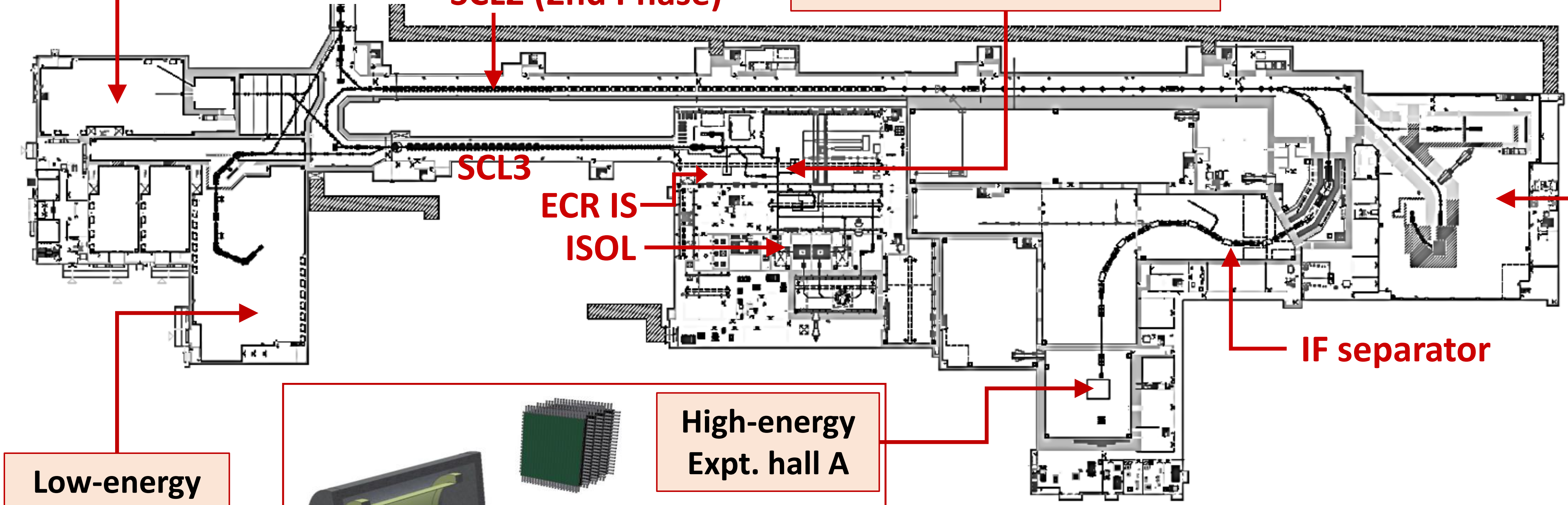

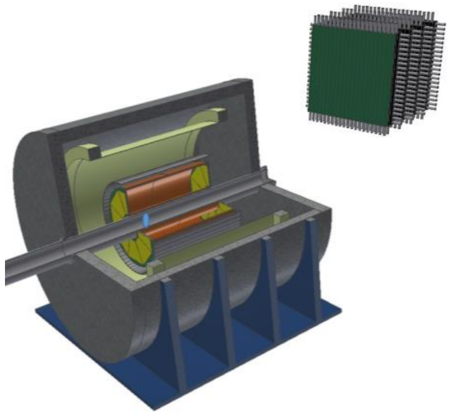

- SIB: ECR IS→SCL3→SCL2→IF(w/o target)
- RIB (ISOL): ISOL→SCL3→SCL2→IF(w/o target)
- RIB (IF): ECR IS→SCL3→SCL2→IF
- **RIB (ISOL+IF): ISOL→SCL3→SCL2→IF**

Overview of LAMPS

- **L**arge **A**cceptance **M**ulti-**P**urpose **S**pectrometer
  - Beam energies up to 250 MeV/u for ^{132}Sn with high intensity
  - Comprehensive detector system to investigate EoS and symmetry energy
  - All detector components and magnet were already developed, manufactured, and assembled.
  - Integration and commissioning of the whole LAMPS system is being planned at the end of 2022.

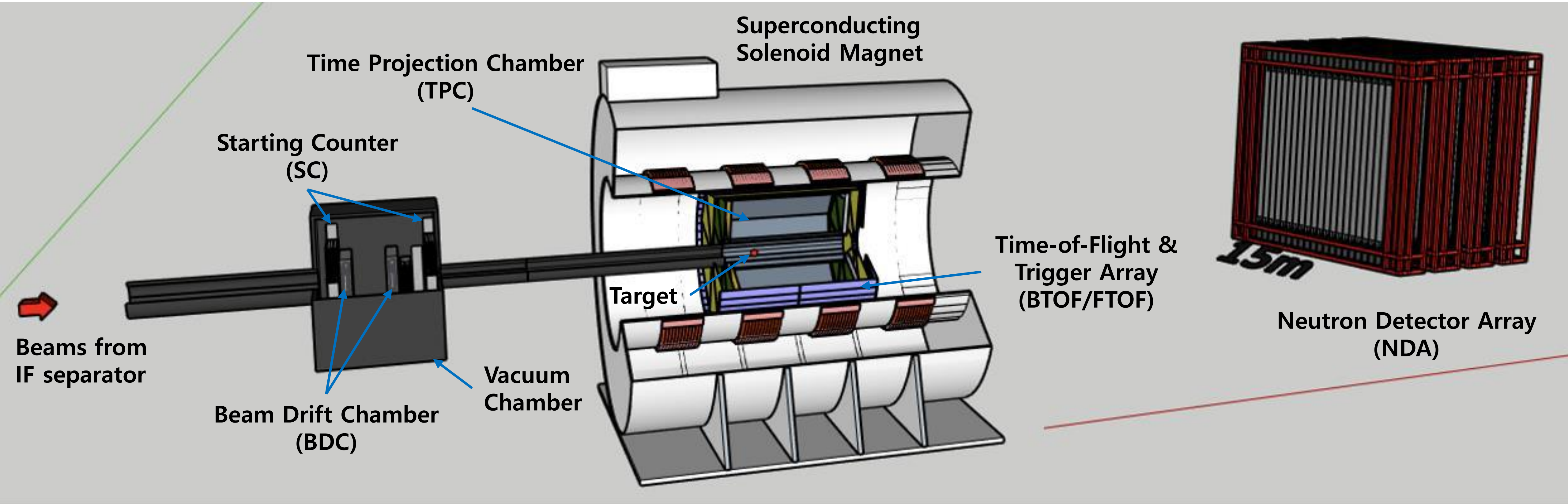

TPC: Performance test with prototype

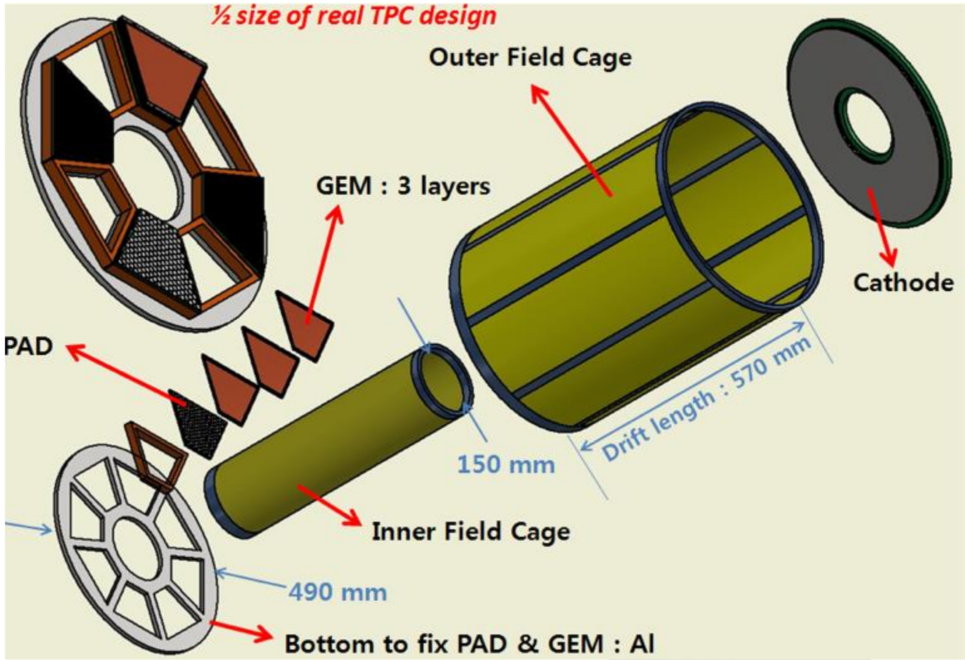

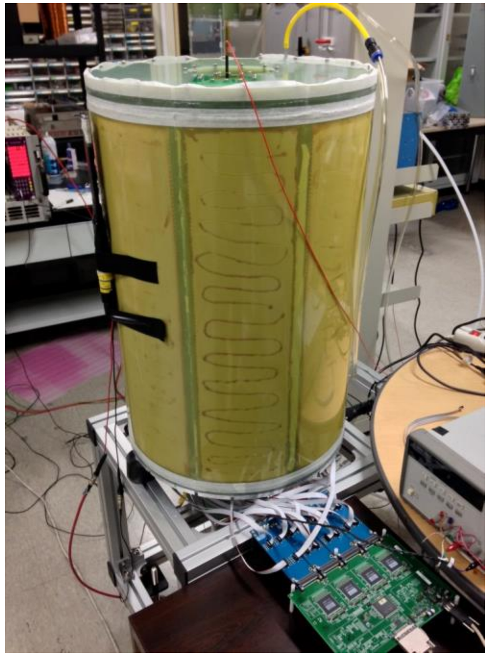

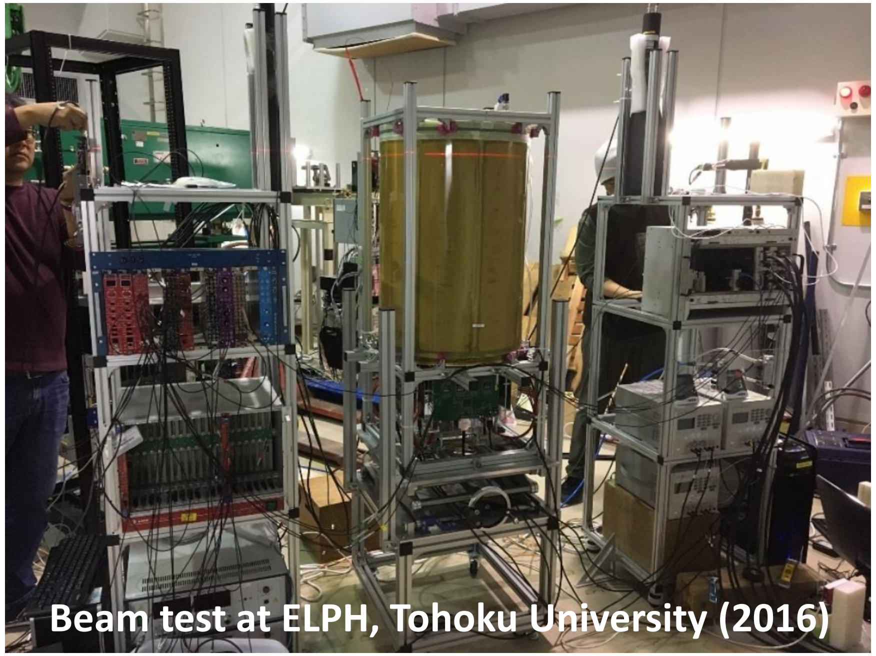

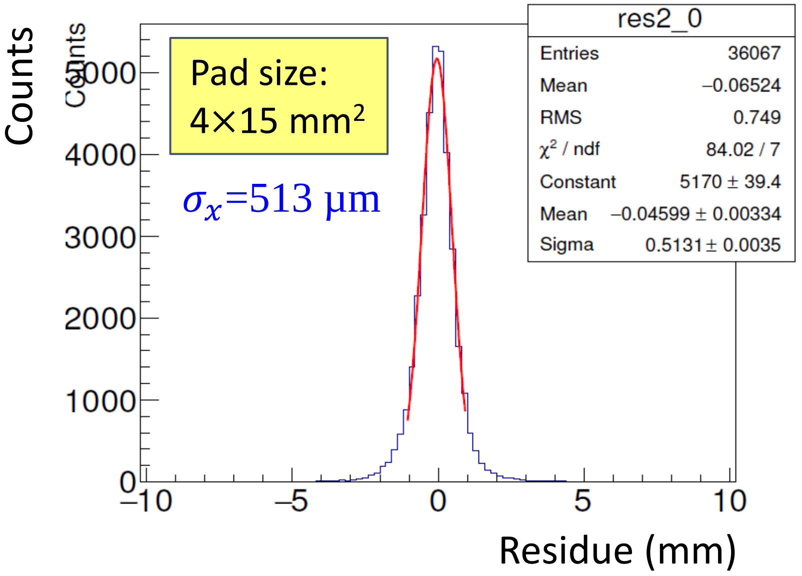

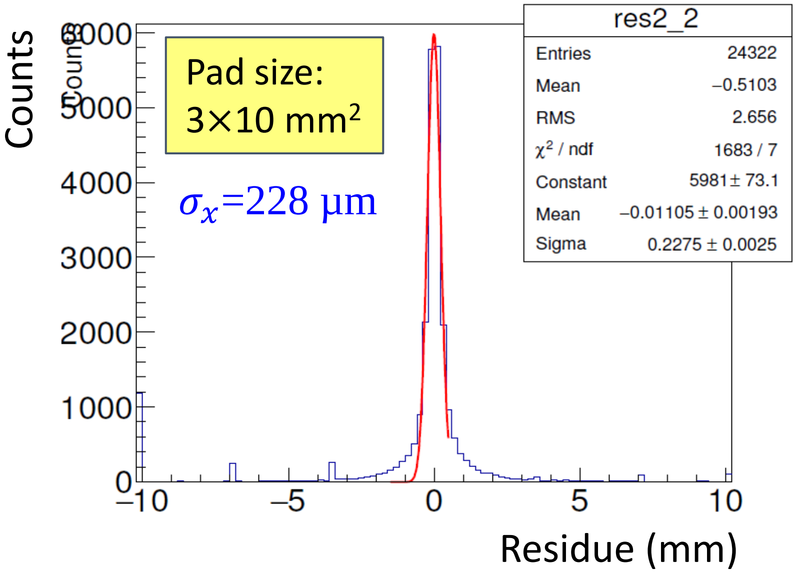

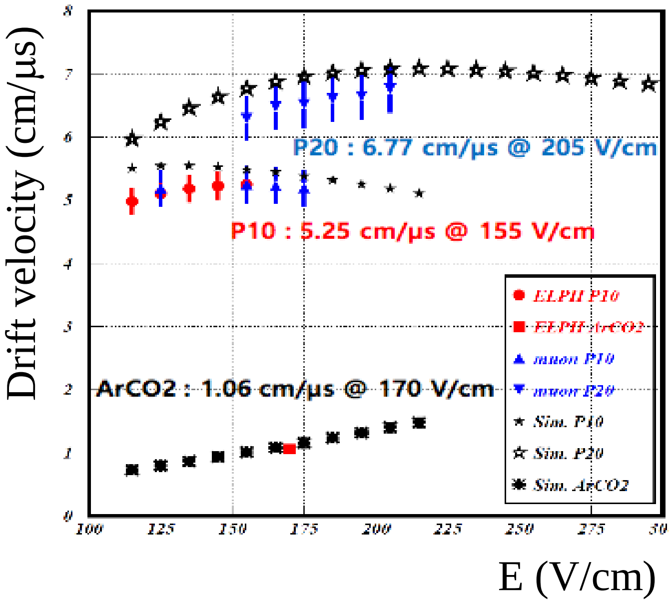

TPC: Construction of real detector

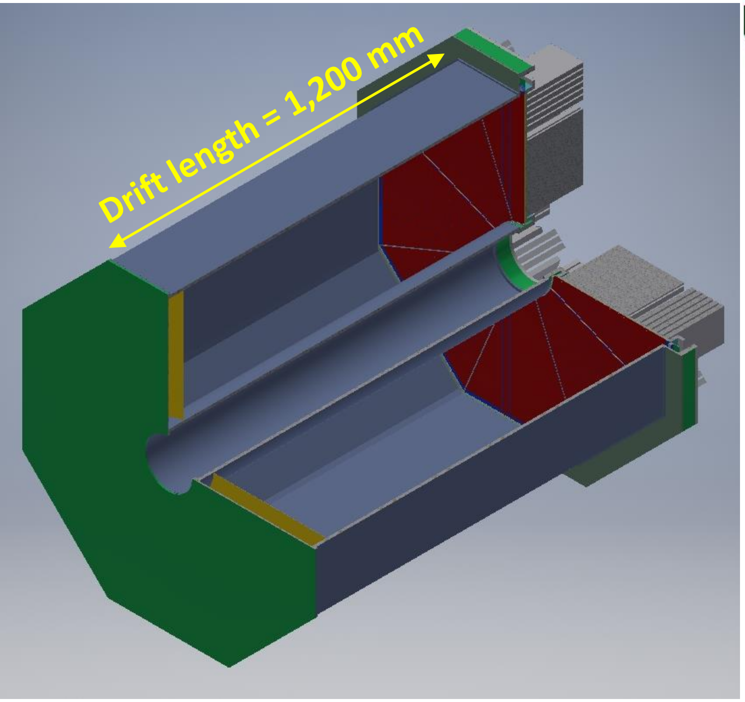

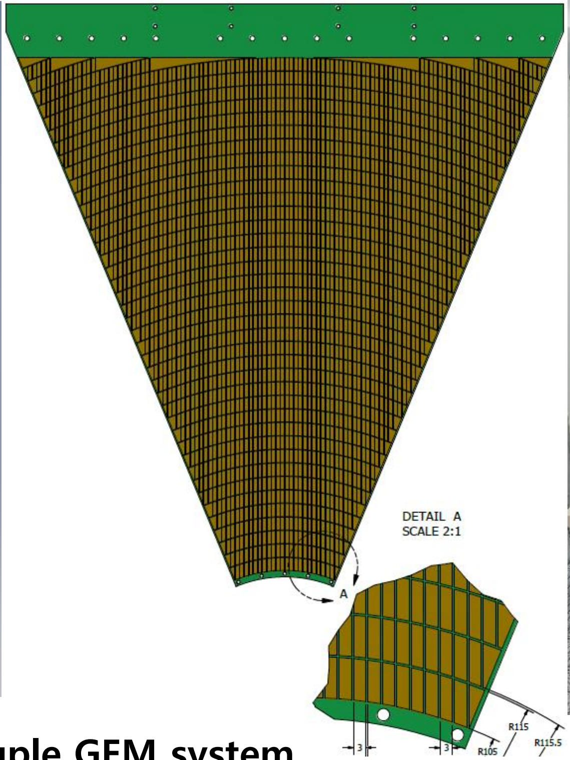

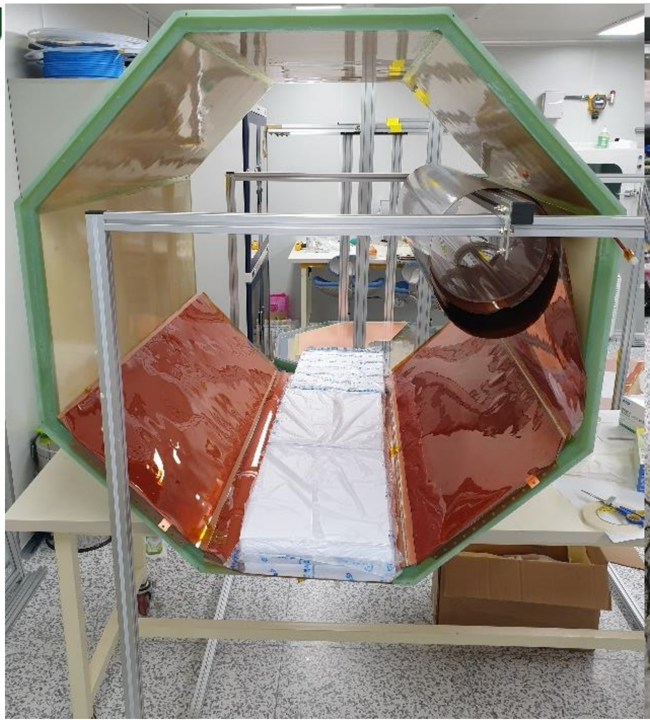

- Pad Dim.: 3×10 mm^2
- Ch. #: 2,618/sector × 8 sectors = 21,584
- FEE (GET electronics): 11 AsAD/sector × 8 sectors = 88 AsAD

Quadruple GEM system

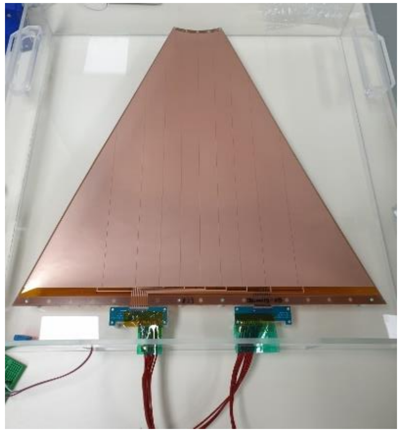

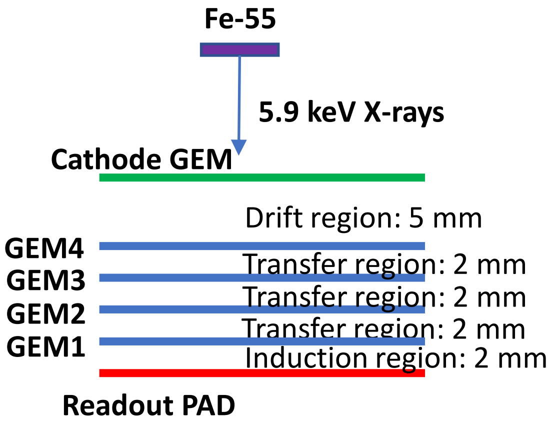

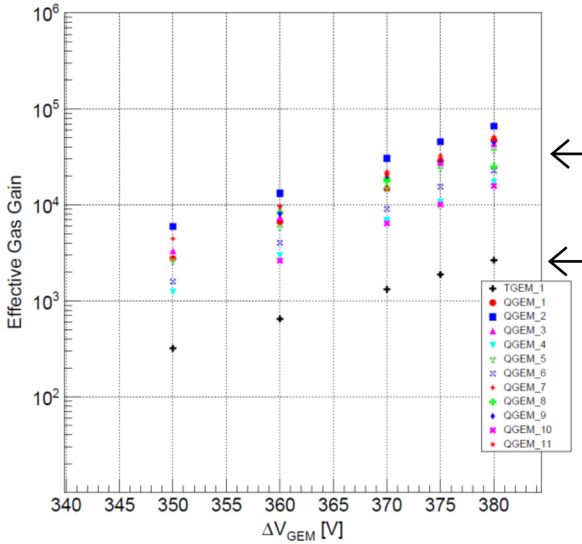

← Quadruple GEM

← Triple GEM

TPC: Drift velocity with cosmic rays

- Cosmic muon trigger
  - Coincidence of two scintillators (scintillator size: 20 x 20 cm^2 each)
  - Trigger position : 30, 60 and 90 cm
  - Measured drift field points: 115, 125 and 135 V/cm

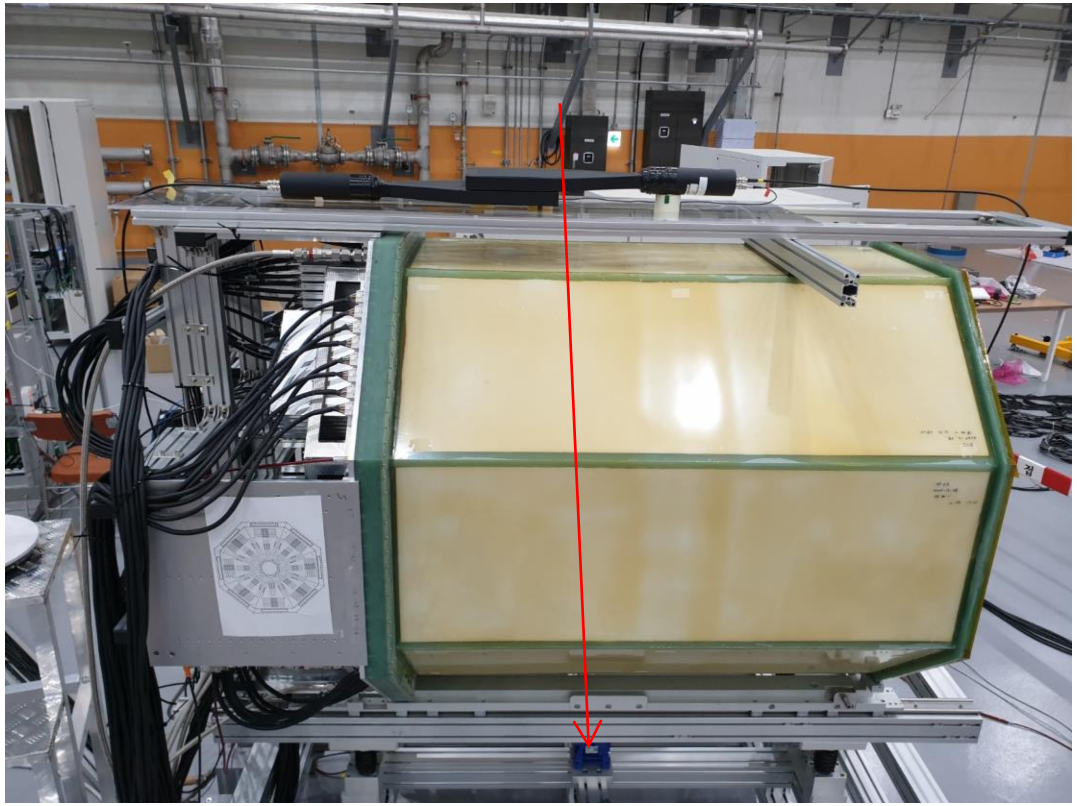

Drift velocity data (preliminary)

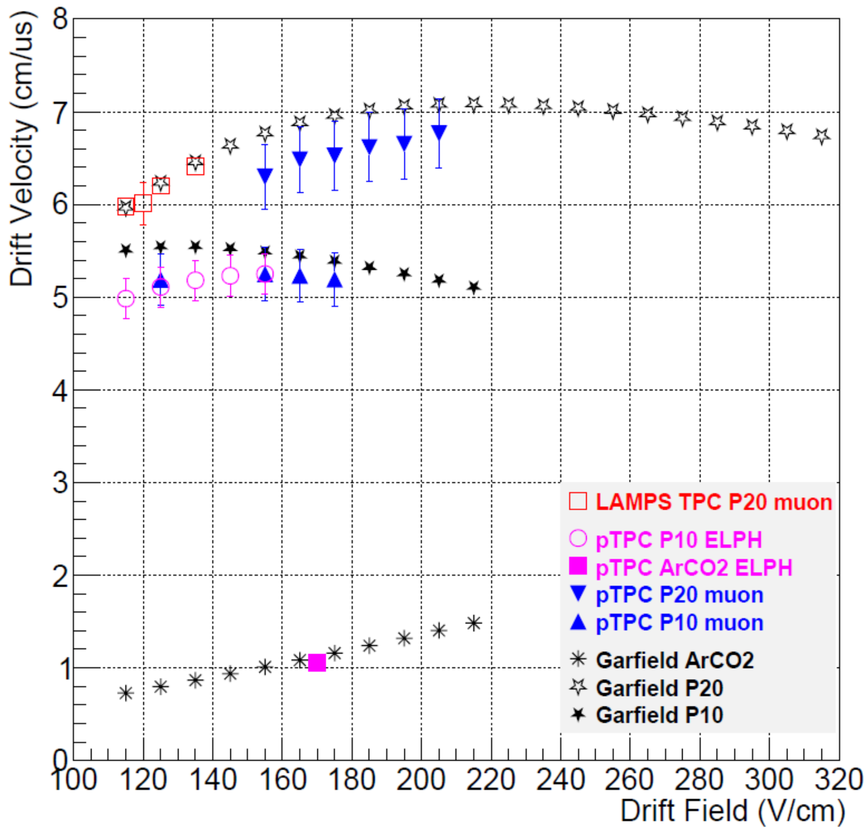

Neutron Detector Array (NDA): Structure

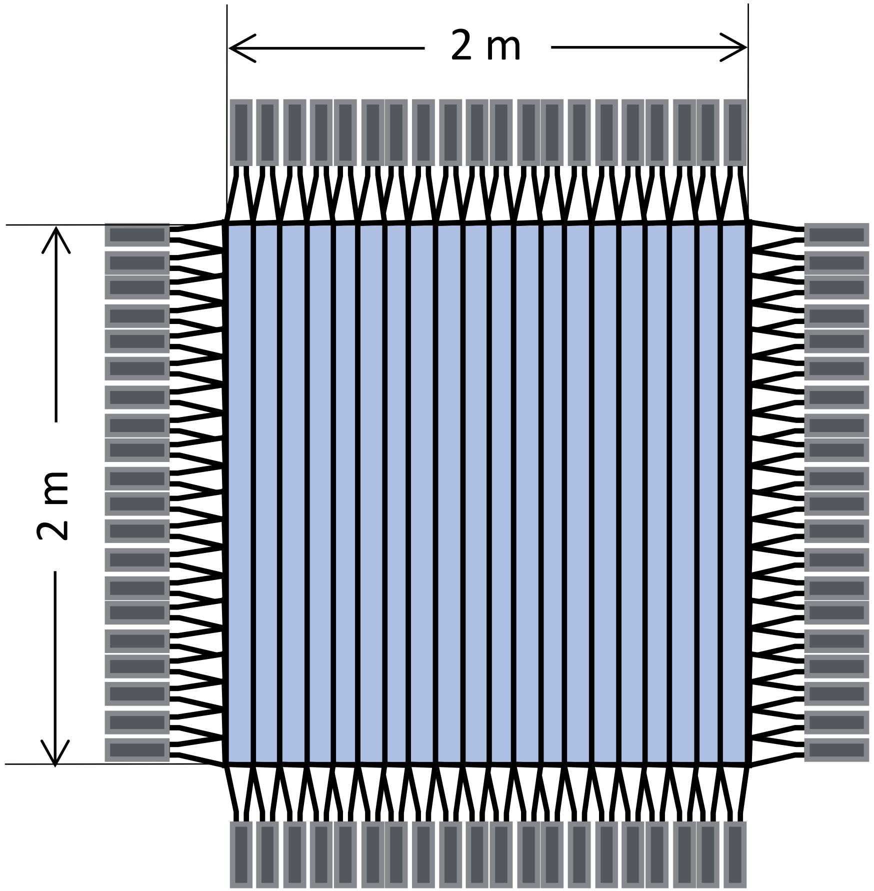

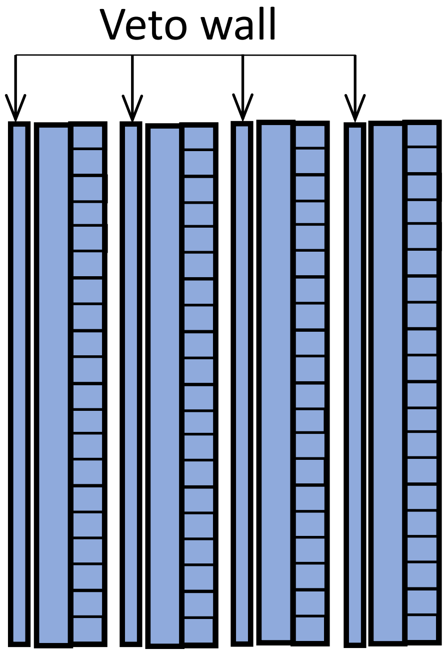

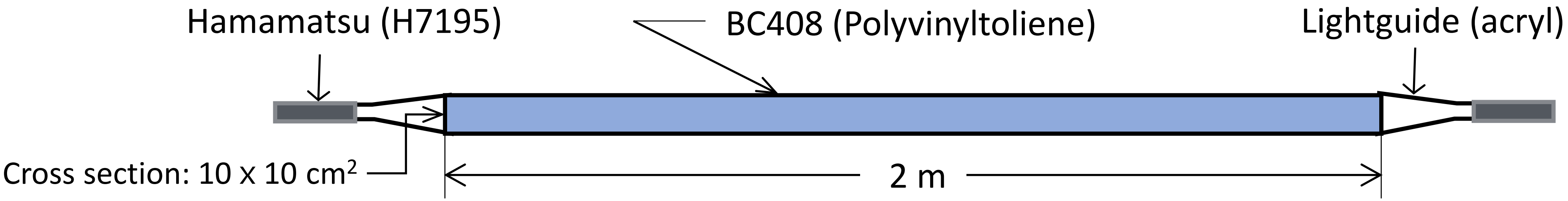

NDA: Performance test with prototype

Beam test at RCNP (2016)

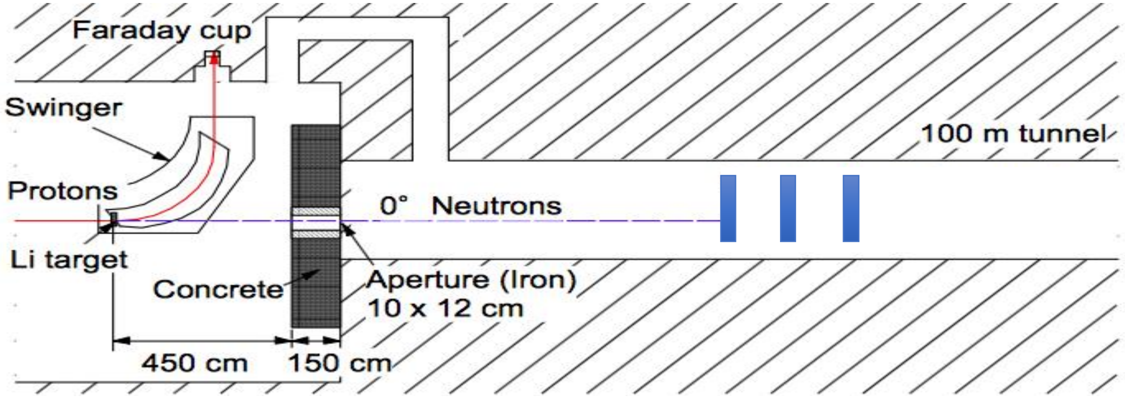

- Beam specifications
  - Production reaction: p+^{7}Li → n + ^{7}Be
  - Neutron beam flux: 1×10^{10} n/sr/μC
  - Neutron energy: 65 and 392 MeV
  - Background neutrons above 3 MeV is < 1% [NIMA 629, 43 (2011)]

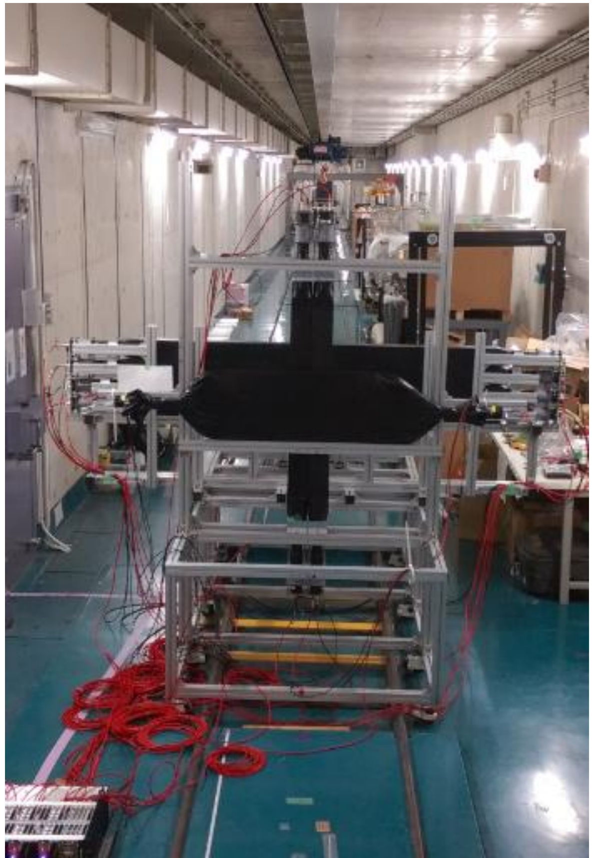

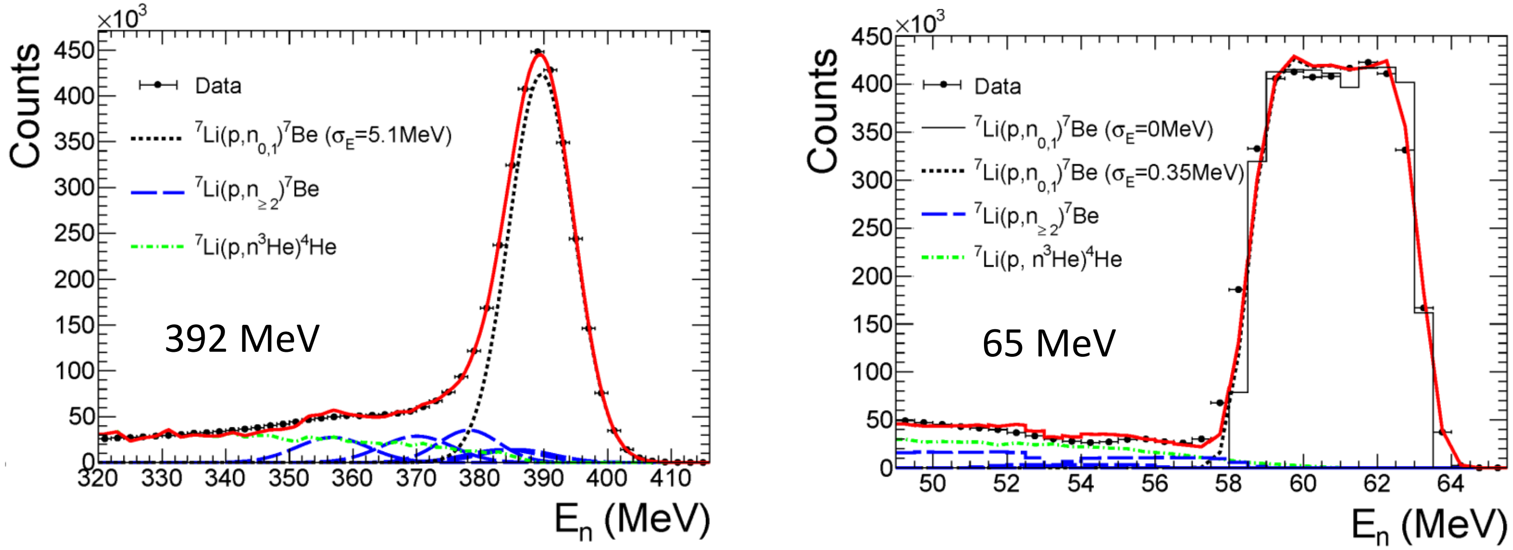

- Significant energy-loss effect in the Li target at 65 MeV
- Low-energy background dominated by the 3-body decays, $^7\mathrm{Li}(p, n\ ^3\mathrm{He})\ ^4\mathrm{He}$, etc.
- Energy resolution (FWHM): 3.1% @ 392 MeV, 1.3% @ 65 MeV

NDA: Construction

- Installation of all modules in the frame at the Sejong campus of Korea University in Dec. 2018.
- The full system was dissembled and transported to the RAON site in Mar. and assembled again in Sept. in 2022.
- The fully assembled system will take the cosmic rays again for testing the performance.


Assembled detector system at the Sejong Campus of Korea Univ.

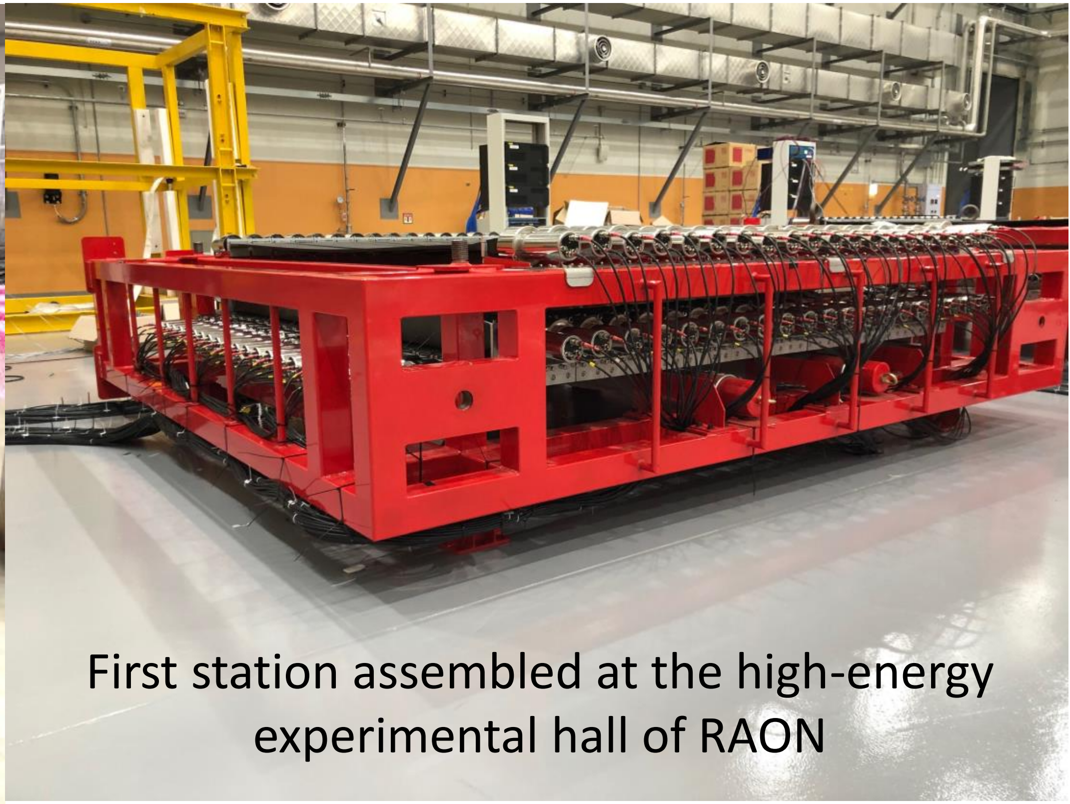
First station assembled at the high-energy experimental hall of RAON

Time-Of-Flight/Trigger Arrays (BTOF/FTOF)

- Number of scintillators & dimensions:
  - BTOF: (48) 1500 X 90 X 10 mm^3 each
  - FTOF: (48) 500 X (90, 24) X 5 mm^3 each
- MPPC readout from both ends
- Installation completed in 2022
- The performance test with cosmic muons is in progress.

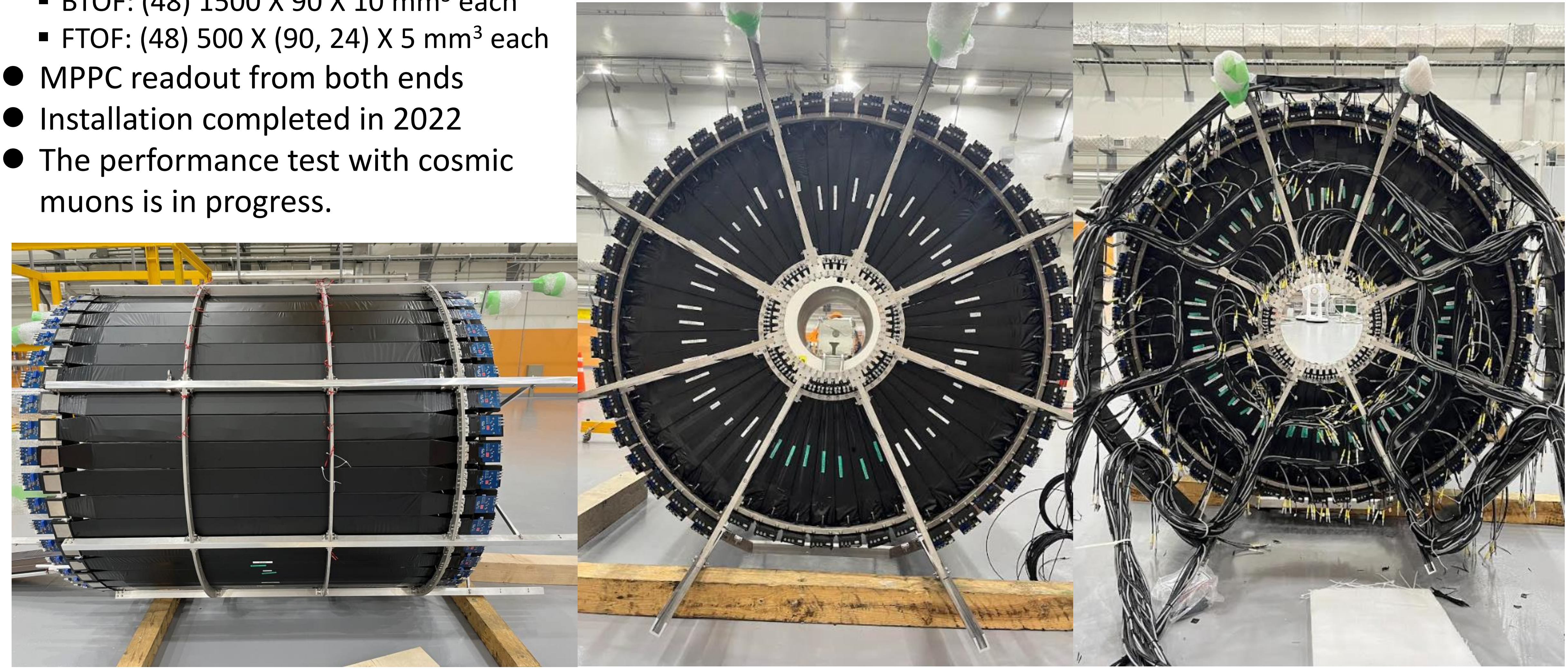

Beam Drift Chamber (BDC)

Parameter	Value
Anode wire	ϕ 20 μm Au-W
Potential wire	ϕ 80 μm Cu-Be or Au-W
Cathode	2 μm-thick Al-mylar, 9 layers
Cell size	5 mm (max. drift length 2.5 mm)
Active area	170 x 170 mm^2
Anode configuration	XX'YY'XX'YY', 8 layers
Number of channel	256 (32 wires/plane, 8 planes)
Operation gas	i-C_4H_{10} below 1 atm P10 (Ar 90% + CH_4 10%) at 1 atm
High voltage	2 channels for cathode & potential wires
Readout	ASD(RP-2125)+TDC(V1190A)+QDC(V792)
Body dimension	490(L) x 360(H) x 100(W) mm^3
Beam window (variable)	12 μm Al-mylar (up to 20 kPa) 50 μm Al-mylar (up to 50 kPa)

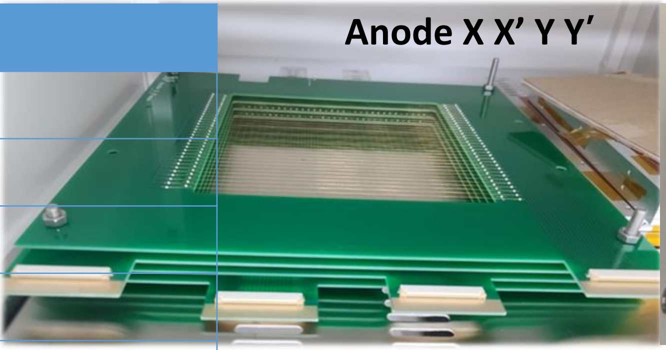

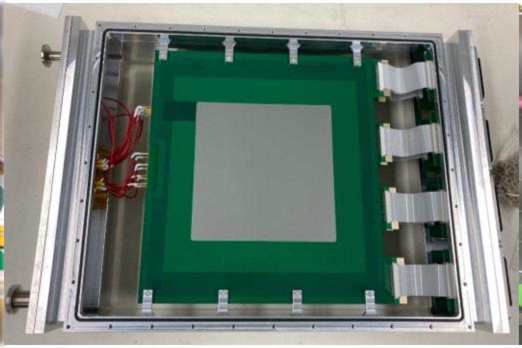

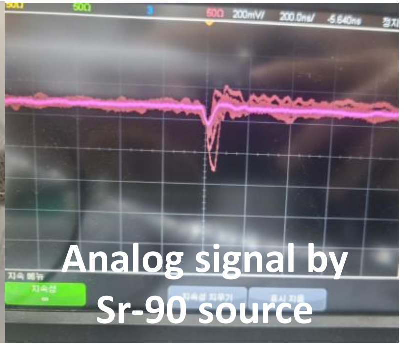

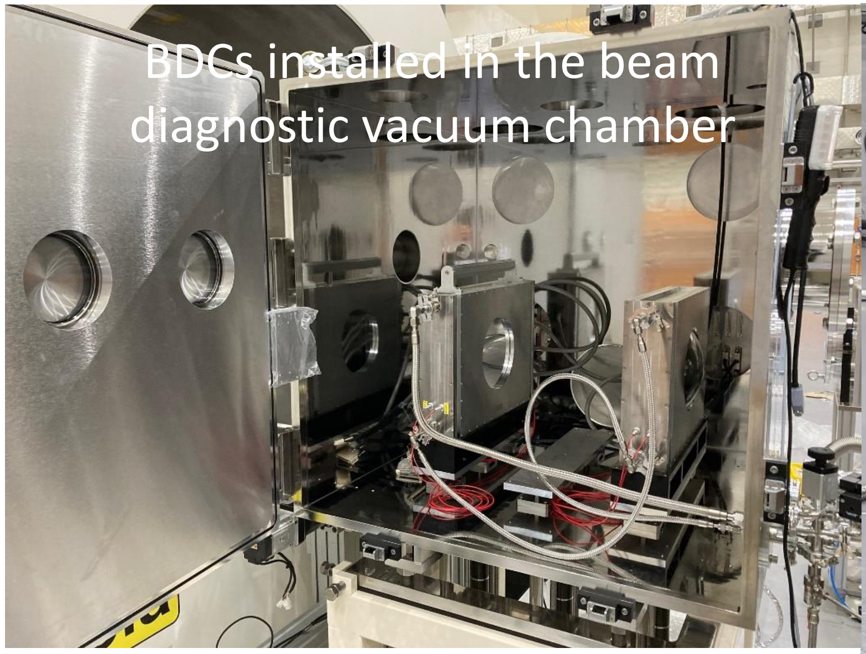

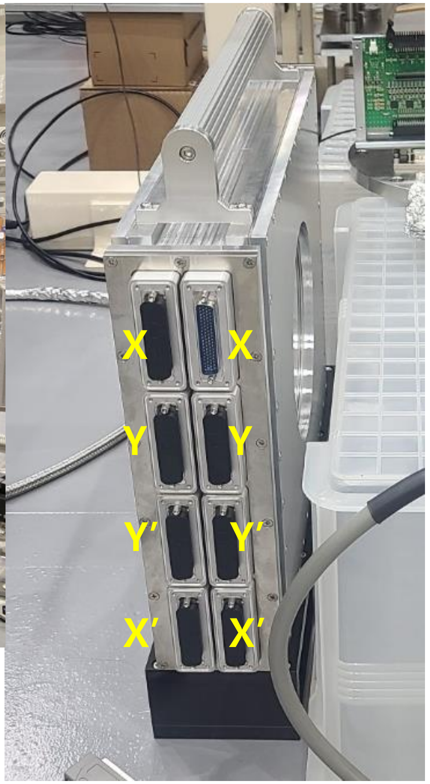

- HV & vacuum tests completed
- Preliminary results with the source demonstrated that the time resolution was ~80 ps in σ (Goal: 100 ps).

Starting Counter (SC)

- Primary function
  - Providing an accurate reference time ($\sigma_t \lesssim 100$ ps) for entire experiment when actual beams arrive.
- Structure & dimensions
  - Two sets of (1 SC + 4 Veto counters)
  - SC: 210 X 210 X 0.2 mm^3 (Active area: 200 X 200 mm^2)
  - Veto: 410 X 210 X 5 mm^3 (Adjustable area)
- Material
  - SC & Veto: EJ-230 polytoluene-based scintillator
  - Lights collected by MPPC on a sensor board
    - 2 sensor boards on a SC scintillator & 1 board for Veto
    - 33 MPPCs on a sensor board for SC & 24 MPPCs for Veto
- Electronics
  - Conventional CAEN TDC, QDC for the time and charge information
- Installation & α source (^{241}Am) test
  - Full system installed in the vacuum chamber
  - σ_t ~130 ps → Using two SC's, ~92 ps is achievable.

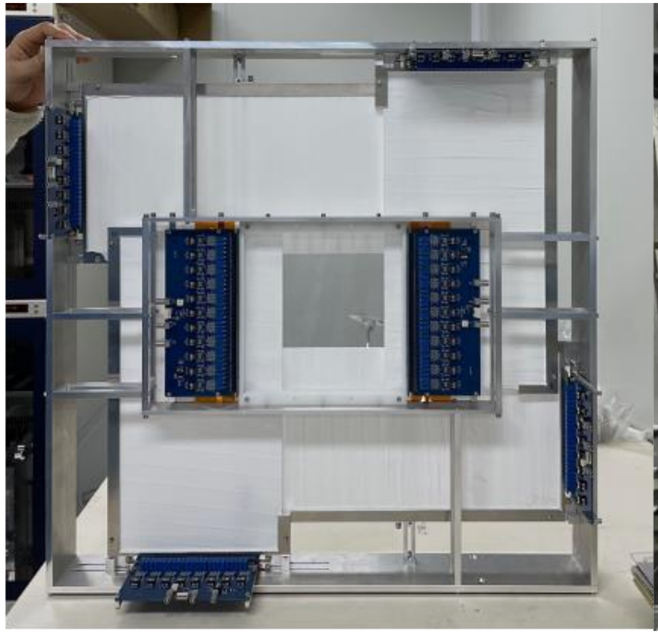

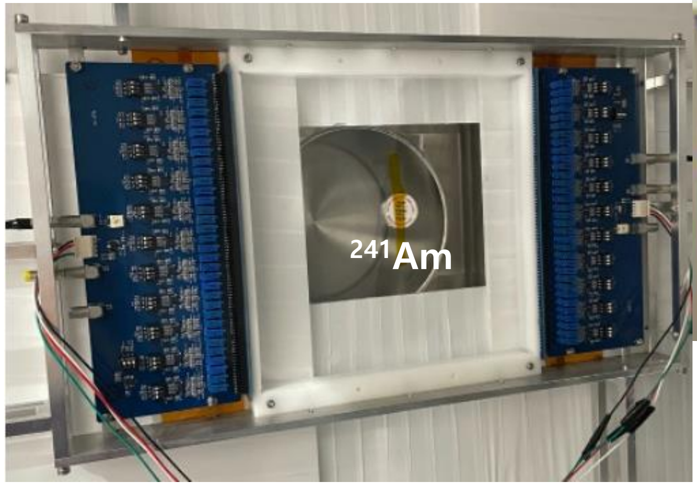

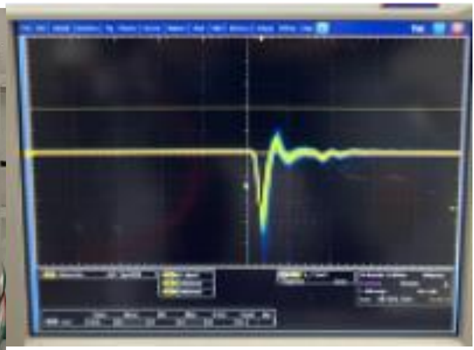

Part 4.

Low-energy detectors

AT-TPC and SC magnet

- Superconducting magnet
  - B_{max} = 1.5 T
  - Diameter & length of the detector space = 60 cm each
  - Conductive cooling
  - Construction done in 2019

- AT-TPC: Construction of prototype
  - # of pads: 64 X 16 = 1024
  - Pad size: 1.9 X 11.9 mm^2 (gap between pads: 0.1 mm)
  - Performance test is on going using cosmic muons & alpha source.
  - Beam test using (α, p) reaction at CRIB is forseen in 2023.

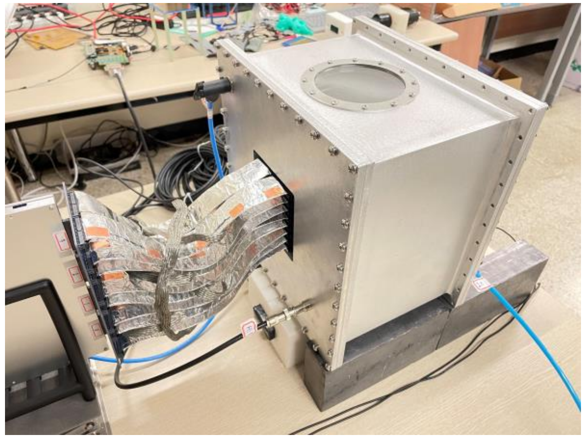

Event display for cosmic muon events

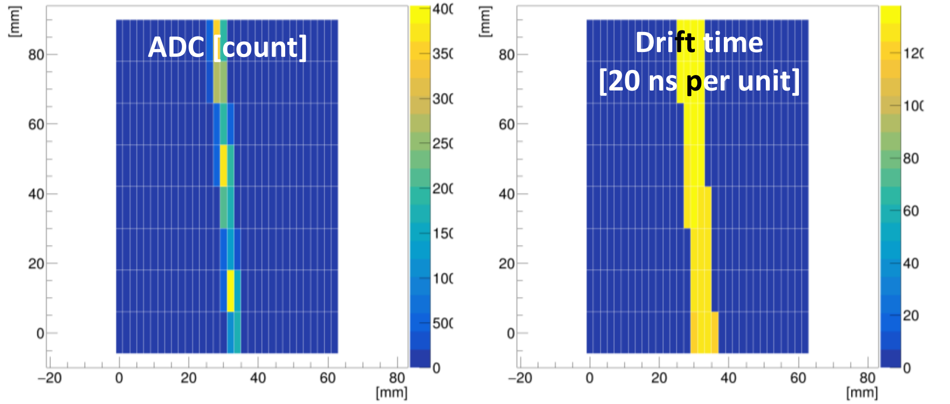

- AT-TPC: Design of real detector

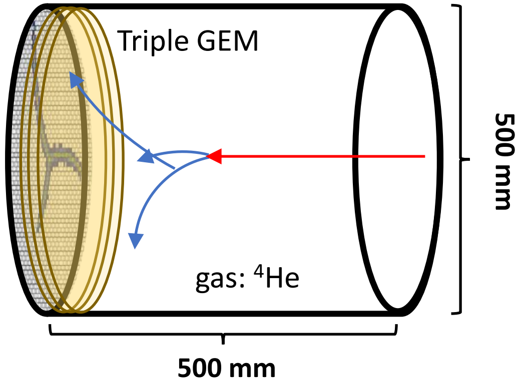

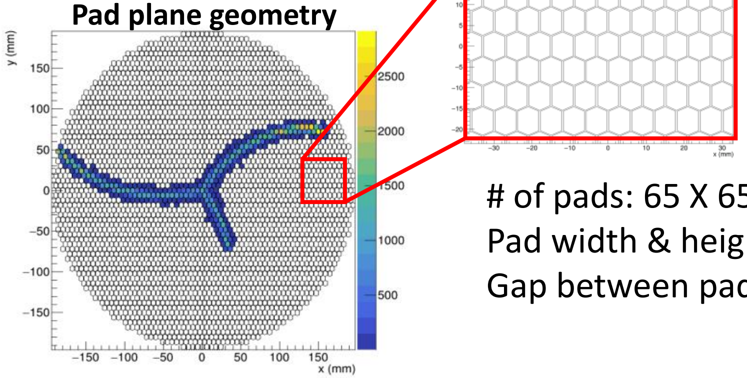

# of pads: 65 X 65 = 3,300
Pad width & height: 6 mm each
Gap between pads: 0.5 mm

KHALA: $LaBr_3$ γ-detector array

- KHALA: Korea High-resolution Array of $LaBr_3$(Ce)
- Total 36 [$LaBr_3$(Ce)+PMT] modules
- R_t < 150 ps (fast timing measurement), R_E< 3.5%
- Formed IDATEN Collaboration = KHALA at CENuM + FATIMA in Europe.
  - IDATEN will perform extensive campaign experiments at RIBF in 2023.

Byul Moon in this Workshop

IDATEN

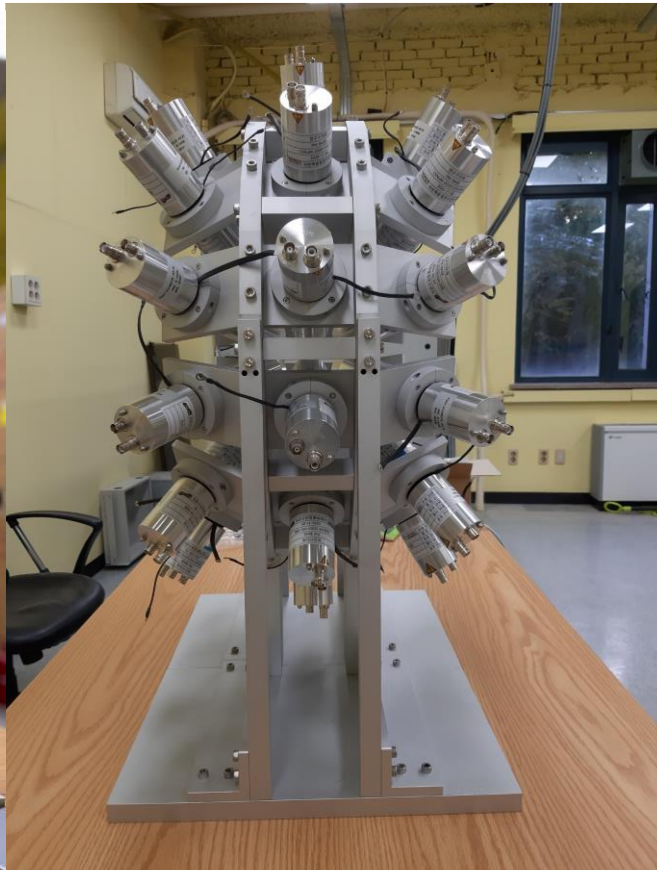

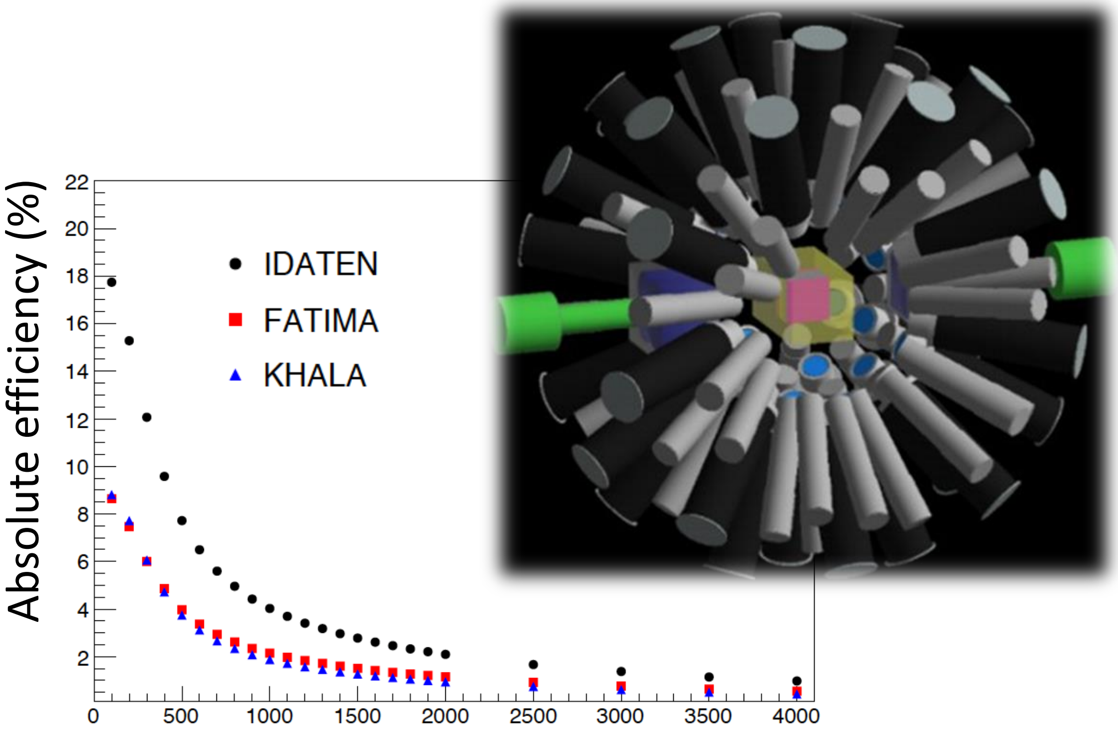

Si+CsI charged particle detector

- FAZIA: A charged-particle detector for heavy-ion collisions at intermediate beam energies
- Each telescope consists of Si_1+Si_2+CsI with cross-sectional dimensions of 2×2 cm^2.
- New Si detectors and electronics are being developed in Korea.

PID from ^{80}Kr+$^{40\text{-}48}$Ca at 35 AMeV in the IsoFAZIA experiment @ LNS, Catania in 2015

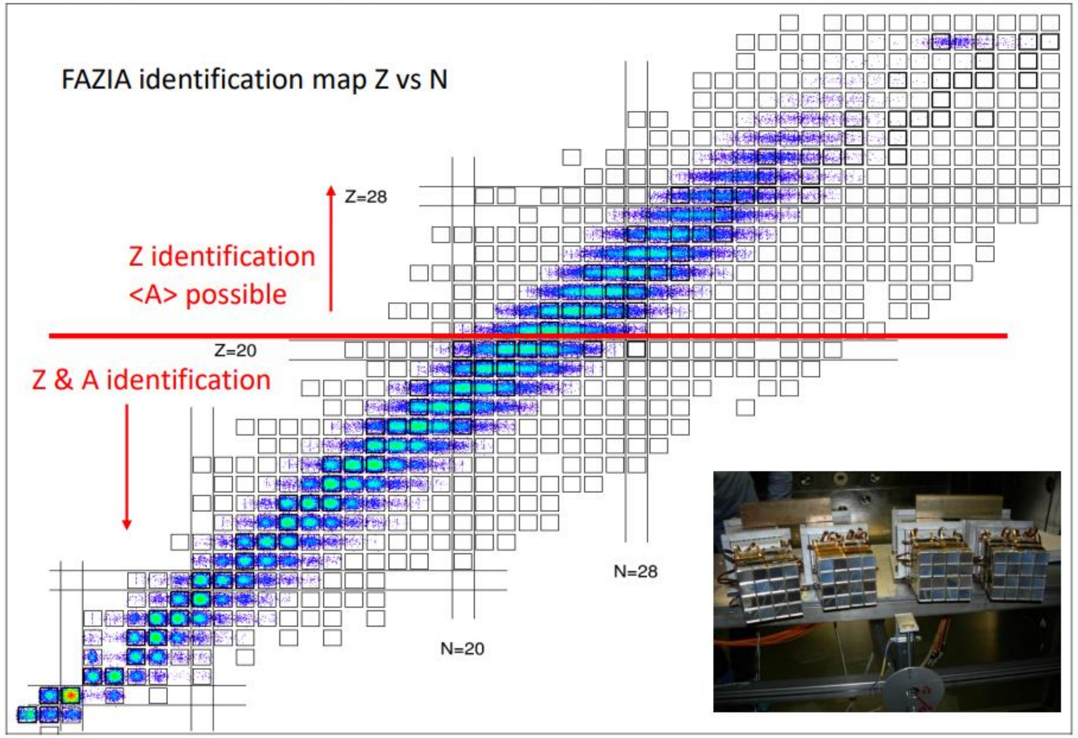

New 750 μm thick Si detector modules (Processed in CiS, Germany)

Si+CsI charged particle detector

- Design and construction of the new (thick) Si detectors
  - The detailed structure, dimensions, and doping profiles are finalized by intense simulations.
  - Low total current, $\mathcal{O}(10\ \mathrm{nA})$, is expected in the working-voltage region.
  - Si wafers are being processed at ETRI in Korea.
- Development of the new FEE card
  - Original schematics were provided by the FAZIA Collaboration.
  - Several changes were implemented for more effective functioning.
- The next step is to design and produce the 150 μm thick detectors.

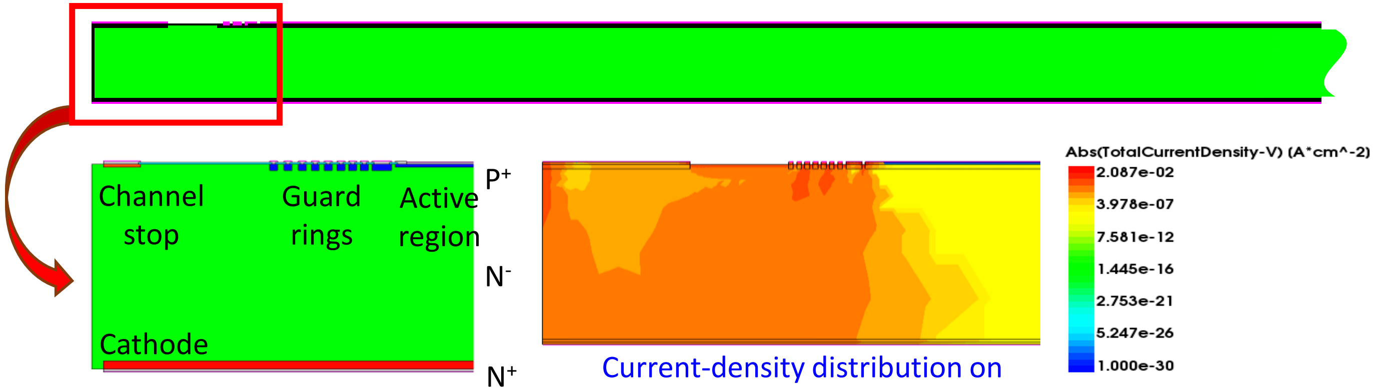

Current-density distribution on the side region from simulation

Assembly of quartetto

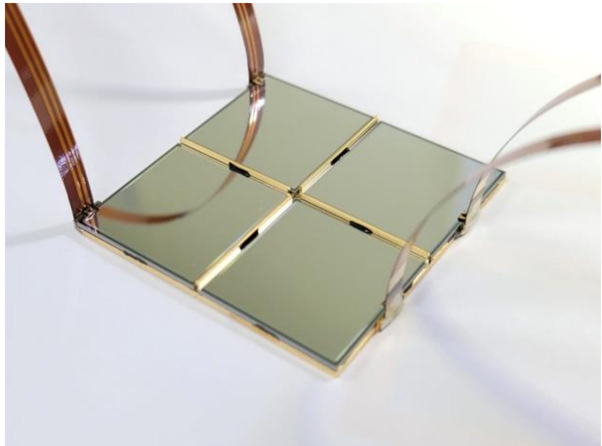

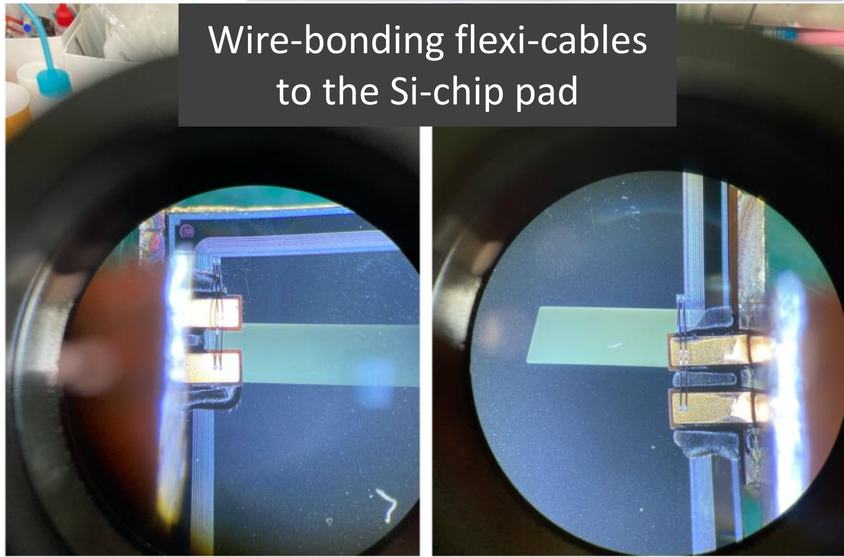

FAZIA / FEE(Front-End Electronics) Old Card

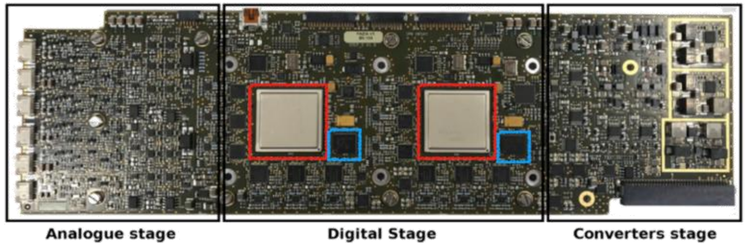

The FAZIA setup, NIMA, Volume 930, 2019, Pages 27-36

New FEE card produced in Korea

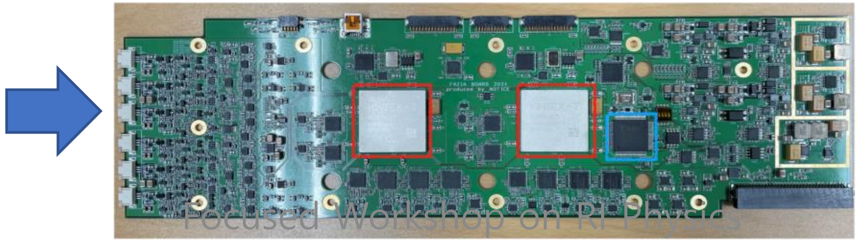

Part 5.

Summary

Summary

- Purpose of LAMPS
  - Detailed investigation of *nuclear equation of state (EoS)*
  - Precise measurement of *symmetry energy* as a function of the baryon density
  - *Structure of exotic nuclei*
- Status of the LAMPS detector system
  - All detector systems were developed, manufactured and assembled.
  - The performance tests with cosmic muons and radiation sources are in progress.
  - *First machine commissioning of the integrated LAMPS system with the trigger electronics is expected in the end of 2022.*
- Plan
  - In the beginning we will concentrate on the low-energy experiments because the high-energy beams from RAON will be available in 2029 or later.
  - We will have a meeting soon to discuss what to do with LAMPS until the high-energy beams are available.